Volume 5 | Number 21 | 7 June 2017 | Pages 10051–10724

Journal of Materials Chemistry A

Materials for energy and sustainability

rsc.li/materials-a

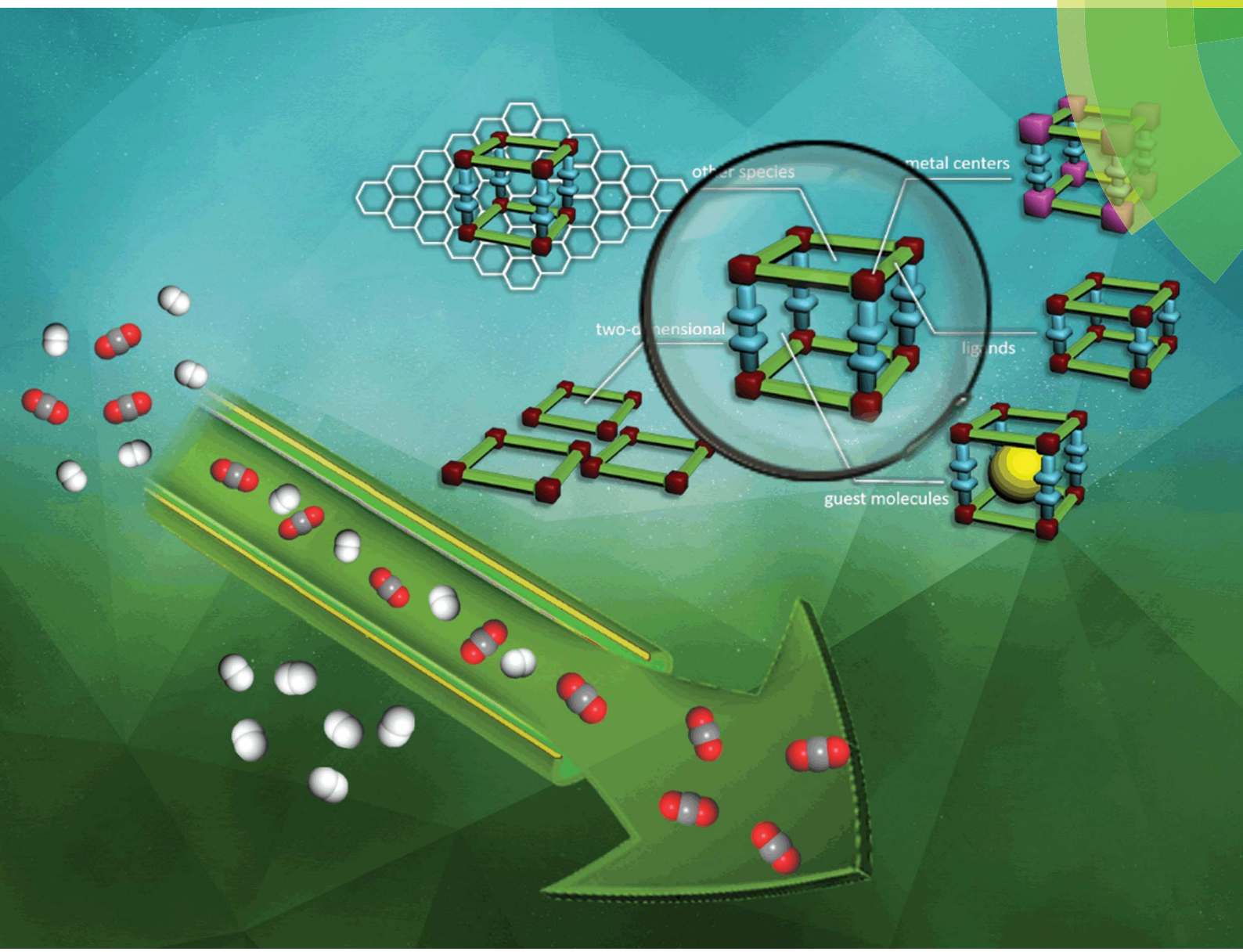

ISSN 2050-7488

ROYAL SOCIETY OF CHEMISTRY

REVIEW ARTICLE

Daofeng Sun *et al.*

Recent advances and challenges of metal–organic framework membranes for gas separation

Journal of Materials Chemistry A

REVIEW

View Article Online
View Journal | View Issue

Cite this: J. Mater. Chem. A, 2017, 5, 10073

Recent advances and challenges of metal–organic framework membranes for gas separation

Zixi Kang, Lili Fan and Daofeng Sun *

Gas separation is one of the most critical and challenging steps for industrial processes, and metal–organic framework (MOF) membranes are potential candidates for this application. This review mainly focuses on the recent advances in improving the performance of MOF membranes, involving the issues faced with MOF designation and growth for practical applications. First, we discussed three strategies for permeability and selectivity enhancement of MOF membranes, in terms of obtaining ultra-thin two-dimensional (2D) MOF nanosheets, fine-tuning the pore size of the MOF framework and integrating with other species. Second, we reviewed the recent potential resolutions to the problems of MOF membranes for future practical applications including scale-up preparation and stability improvement. Finally, we summarized our work by providing some general conclusions on the state-of-the-art and an outlook on some development directions of molecule-sieving membranes.

Received 6th February 2017
Accepted 21st March 2017

DOI: 10.1039/c7ta01142c

rsc.li/materials-a

Introduction

The separation of mixtures is one of the critical steps in the chemical industry and can account for as much as half the total energy of many industrial processes.[1] Among all the mixtures, the separations of gas mixtures are of great importance for industrial processes[2] such as in hydrogen purification (H_2/N_2, H_2/CO, H_2/CO_2, H_2/hydrocarbons),[3] air separation (N_2/O_2),[4] natural gas sweetening (CO_2/CH_4),[5,6] CO_2 capture (CO_2/air, CO_2/H_2),[7] and hydrocarbon separation (olefins/paraffins, linear/branched isomers, *etc.*).[8,9] For these mixtures, gas pairs composed of molecules of a similar size or physical property are particularly difficult to be separated. Membrane separation is a promising technique that has been put forward in an attempt to address these energy and environmental challenges, and thus has undergone rapid development over the past few decades.[3,10–14] Compared with traditional gas separation techniques such as PSA/TSA operation, membrane-based gas separation technologies offers greater potential in terms of their lower energy consumption, smaller carbon footprint, and ease of operation. Among the diverse materials used so far for membrane preparation, polymers and zeolites have been most extensively investigated. Polymer membranes have been widely used in industrialized gas separation processes owing to their many advantages, such as ease of processing and low operation cost.[15] However, polymers suffer from a trade-off between the desirable permeability and selectivity for gas separation.[16,17]

College of Science, China University of Petroleum (East China), Qingdao, Shandong, 266580, People's Republic of China. E-mail: lilifan@upc.edu.cn

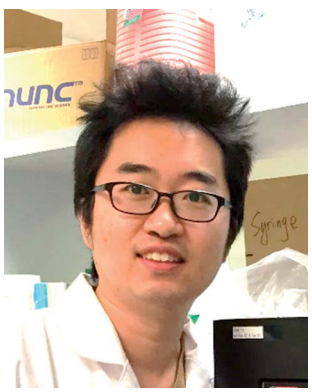

Dr Zixi Kang completed his PhD (2013) degrees in Inorganic Chemistry under the supervision of Prof. Shilun Qiu from Jilin University in China, and joined the National University of Singapore to work with Dr Dan Zhao as a postdoctoral research fellow during 2014–2015. Currently, he works in the College of Science, China University of Petroleum (East China), as a lecturer. His work is focused on multifunctional metal–organic framework materials and membranes for applications in adsorption and separation.

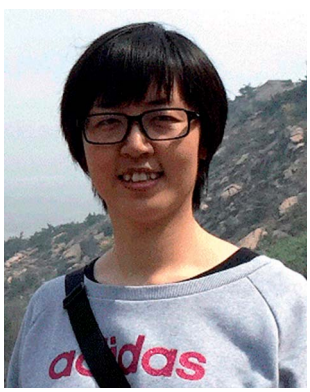

Dr Lili Fan completed her PhD (2014) degree in Inorganic Chemistry under the supervision of Prof. Shilun Qiu from Jilin University in China. She then worked with Prof. Xiangdong Yao from Griffith University as a visiting scholar during 2013–2014. Now, she works in the College of Science, China University of Petroleum (East China), as a lecturer. Her work is focused on functional porous materials applied in the field of energy and the environment.

Indeed, most polymer membranes only offer high selectivity but low permeability, which means larger areas of the membranes get used. Furthermore, polymer membranes with high permeability usually exhibit lower selectivity due to their wide range of pore sizes. On the other hand, zeolite membranes possess a uniform pore size, which can overcome the disadvantages of polymer membranes, and also simultaneously have high permeability and selectivity.[11,18–20] However, zeolite membranes are limited in their chemical tailorability for enhancing their separation selectivity.[12,21]

As an emerging class of porous crystalline materials, metal–organic frameworks (MOFs) have received considerable attention for gas storage/separation, heterogeneous catalysis, chemical sensing, *etc.*[22] In the pioneer studies, several famous MOF structures, such as MOF-5, HKUST-1, and the ZIF series, were successfully prepared into membranes for different applications of gas separation processes.[23–33] A number of reviews have summarized the fabrication of MOF membranes and their separation performances in different fields. In the themed issue of Chemical Society Reviews on MOFs, Prof. Zhou and Fischer introduced selective gas adsorption and separation utilizing MOFs and widely covered MOF film preparation.[34,35] Prof. Caro and Tsapatsis discussed the conceptual similarities and practical differences between zeolite and MOF membranes.[36] Prof. Keskin summarized the experimental studies and computational modeling methods involving MOF-based mixed-matrix membranes (MMMs).[37] Prof. Qiu provided an overview of the diverse MOF membranes, including current techniques for MOF membrane fabrication and gas and liquid separation applications with different MOF membranes.[38] More recently, a review by Prof. Li focused on the potential applications of water-stable MOFs, including membrane separation.[39] Water-stability is a key issue affecting the potential capability of MOFs in separation applications.

After the initial steps of developing different MOF structures into membranes, recent studies on MOF membranes now focus on the improvement of membrane performance and the issues they face in practical application (Fig. 1). In this review, we intend to focus on these recent advances and the remaining challenges for utilizing MOF membranes for gas separation, particularly MOF design and growth (Table 1). First, we discuss several strategies for enhancing membrane permeability and selectivity, in terms of obtaining ultrathin 2D MOF nanosheets, fine-tuning the pore size of the MOF framework and integrating with other species. Second, we review the recent potential resolutions to problems of utilizing MOF membranes in future practical applications, including issues with the scale-up preparation and the stability improvement. Finally, we round up the review by providing some general conclusions on the state of the art and an outlook on some development directions for molecule-sieving membranes.

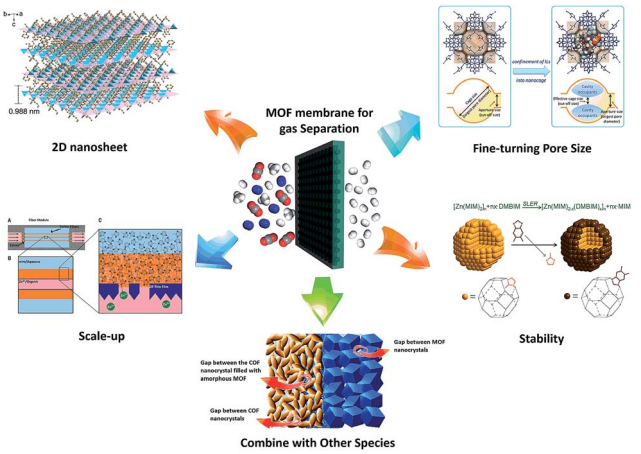

Fig. 1 Recent advances and challenges for metal–organic framework membranes for gas separation. (Adapted with permission from ref. 40–44. Copyright 2014 Science, 2015 Wiley, 2016 American Chemical Society, 2013 RSC.)

Dr Daofeng Sun completed his PhD in Physical Chemistry under the supervision of Prof. Maochun Hong and Rong Cao from the Fujian Institute of Research on the Structure of Matter, Chinese Academy of Science (2003). He worked with Prof. Hongcai Zhou at the University of Miami as a postdoctoral fellow during 2003–2006, before joining Shandong University in 2007. He moved to China University of Petroleum (East China) in January 2013, and now is a full professor of Chemistry. His research interests focus on porous materials.

Recent advances in MOF membranes

MOFs with a high surface area and permanent porosity are more extensive in their variety and multiplicity than any other class of porous materials due to their wonderful designability and flexibility.[45] All of these aspects make MOFs ideal candidate materials for membranes in separation processes. Both the preparation and gas separation applications of MOF membranes have been seen tremendous progress in the last few years. Aimed at obtaining better permeability and selectivity, recent advances in MOF membranes are focused on fabricating 2D MOFs nanosheets, fine-tuning the pore size and integrating with other species in the membrane preparation (Fig. 2). In this section, we discuss these three directions.

2D MOF nanosheets

For many years, researchers have attempted to make artificial membranes with both ultrathin thickness and uniformly distributed pore sizes that can separate molecules effectively. In this regard, 2D microporous nanosheets are the most appropriate building block for this kind of membrane.[70–74] In recent years, numerous attempts have been made to prepare 2D zeolite nanosheets and membranes.[75–78] Prof. Tsapatsis, Prof. Valtchev, and Prof. Mintova carried out pioneering work into different

Table 1 Summary of gas separation performance for the MOF membranes discussed in this review

MOF	Substrate	Highlights	Thickness (μm)	T (°C)	Gas pair	Permeance (mol m^{-2} s^{-1} Pa^{-1})	Separation factor	Ref.
$Zn_2(bim)_4$	α-Al_2O_3 disk	2D nanosheet	0.1	25	H_2/CO_2	7.74×10^{-6}	230	40
CuBDC	MMMs	2D fillers	30–50	25	CO_2/CH_4	2.33×10^{-11}[a]	88.2	46
$Cu_2(ndc)_2dabco$	MMMs	2D fillers	40	35	H_2/CO_2	5.13×10^{-11}	26.7	47
ZIF-8	AAO	ZIF-8/GO seed	0.1	25	H_2/C_3H_8	5.46×10^{-8}	405	48
$Cu_2(BME\text{-}bdc)_2dabco$	Titania disc	Stepwise liquid-phase deposition	1	25	CO_2/CH_4	1.50×10^{-8}	4.5	49
$Ni_2(L\text{-}asp)_2pz$ (JUC-150)	Nickel mesh	Fine-tuning of pore size	20	25	H_2/CO_2	1.83×10^{-7}	38.7	50
CuBTC/MIL-100	Hollow fiber	Metal exchange	20	85	H_2/CO_2 H_2/N_2	1.05×10^{-7}	89.0 (H_2/CO_2) 240.5 (H_2/N_2)	51
ZIF-8/ZIF-67	α-Al_2O_3 support	Heteroepitaxial synthesis	1	RT	C_3H_6/C_3H_8	3.70×10^{-8}	209.1	52
ZIF-90	α-Al_2O_3 disk	Ethanolamine modification	20	325	H_2/CO_2	3.80×10^{-7}	20.4	26
ZIF-90	α-Al_2O_3 disk	APTES modification	20	225	H_2/CO_2	2.83×10^{-7}	21	53
MOF-74 (Mg)	α-Al_2O_3 disk	Ethylenediamine modification	10	25	H_2/CO_2	8.20×10^{-8}	28	54
$Ni_2(L\text{-}asp)_2bpe$	Nickel mesh	*In situ* doping of free linkers	20–30	25	H_2/CO_2	1.00×10^{-6}	24.3	55
ZIF-8	MMMs	ILs as cavity occupants	30	30	CO_2/CH_4 CO_2/N_2	3.65×10^{-9}	38.3 (CO_2/CH_4) 116 (CO_2/N_2)	41
HKUST-1	Copper net	Twin copper source	60	RT	H_2/N_2 H_2/CO_2 H_2/CH_4	1.50×10^{-6}	7 (H_2/N_2) 6.8 (H_2/CO_2) 5.9 (H_2/CH_4)	33
ZIF-8	γ-Al_2O_3 substrate	ZnAl-LDH buffer layer	20	RT	H_2/CH_4	1.40×10^{-7}	12.5	56
ZIF-8	α-Al_2O_3 disk	Conversion of ZnO coating	20	100	H_2/CO_2 H_2/CH_4	5.50×10^{-8}	7.8 (H_2/CO_2) 12.5 (H_2/CH_4)	57
HKUST-1	Free-standing	Conversion of CHNs	5	RT	H_2/N_2 H_2/CO_2 H_2/CH_4	1.50×10^{-6}	4 (H_2/N_2) 6.1 (H_2/CO_2) 5 (H_2/CH_4)	58
ZIF-8	α-Al_2O_3 disk	GO for fixing the inter-crystal gap	25	250	H_2/N_2 H_2/CO_2 H_2/CH_4 H_2/C_3H_8	1.50×10^{-6}	90.5 (H_2/N_2) 14.9 (H_2/CO_2) 139.1 (H_2/CH_4) 3816 (H_2/C_3H_8)	59
$Zn_2(bdc)_2dabco$	Porous SiO_2	Combined with COF layer	100	RT	H_2/CO_2	4.35×10^{-8}	12.6	42
ZIF-8	MMMs	Scale-up, hollow fiber	7–11	35	C_3H_6/C_3H_8	9.16×10^{-10}	27.5	60
ZIF-8	Hollow fiber	Inner side of hollow fiber	9	25	H_2/C_3H_8	3.70×10^{-6}	328	43
ZIF-7	Hollow fiber	Inner side of hollow fiber	2.4	35	H_2/N_2 H_2/CH_4	2.20×10^{-9}	35.1 (H_2/N_2) 34.6 (H_2/CH_4)	61
ZIF-93	Hollow fiber	Inner side of hollow fiber	2	100	H_2/CH_4	1.10×10^{-8}	97	62
ZIF-8	Porous SiO_2	Electrospinning technique	60	RT	H_2/N_2 H_2/CO_2 H_2/CH_4	1.50×10^{-6}	4.9 (H_2/N_2) 7.3 (H_2/CO_2) 4.8 (H_2/CH_4)	63
ZIF-7	α-Al_2O_3 disk	Electrospray deposition	4.5	150	H_2/CO_2	3.05×10^{-7}	18.3	64
ZIF-8	α-Al_2O_3 disk	LPE method	0.5	50	CH_4/C_4H_{10}	1.34×10^{-9}	16	65
HKUST-1	α-Al_2O_3 disk	Step-by-step spray	0.5	RT	H_2/CO_2	1.00×10^{-7}	7	66
ZIF-8	α-Al_2O_3 disk	On-stream stability test	2.5	35	C_3H_6/C_3H_8	1.00×10^{-7}	30	67
$Co_2(dobdc)$	MMMs	Plasticization resistance	40–70	35	C_2H_4/C_2H_6	1.68×10^{-9}	3.9	68
$Ni_2(dobdc)$	MMMs	Plasticization resistance	40–70	35	C_2H_4/C_2H_6	2.59×10^{-9}	4.2	68
MAMS-1	AAO	2D, thermo-switchable	0.04	20–120	H_2/CO_2	1.88×10^{-6}	235	69

[a] Calculated based on the permeability and membrane thickness.

zeolite structures.[79–82] MOFs with abundant porous structures are suitable candidates to serve as diverse sources for MOF-based nanosheets. Keeping the MOF structure and narrow thickness distribution are key issues during the preparation to ensure the success of obtaining high-quality MOF nanosheets.

Before making into membrane materials, some attempts were made to prepare MOF nanosheets. Generally, there are two approaches to obtain 2D MOF nanosheets, namely top-down and bottom-up. Top-down approaches refer to applying mechanical force, such as ball-milling or sonication, on bulk MOF crystals to yield exfoliated MOF nanosheets.[83,84] For the top-down method, the first exfoliated MOF research was reported by Prof. Zamora, who used probe sonication to break the π–π stacking between layers.[85] MOF nanosheets with a thickness of 5 ± 0.15 Å were obtained after the sonication treatment, referring to a single atom layer. In the work of Prof. Xu and co-workers, they discussed the solvent effect on the exfoliation of MOF-2, stating that acetone is suitable.[84] On the other hand, bottom-up approaches denote the direct synthesis of 2D MOF nanosheets, which includes adjusting the solvent, contact

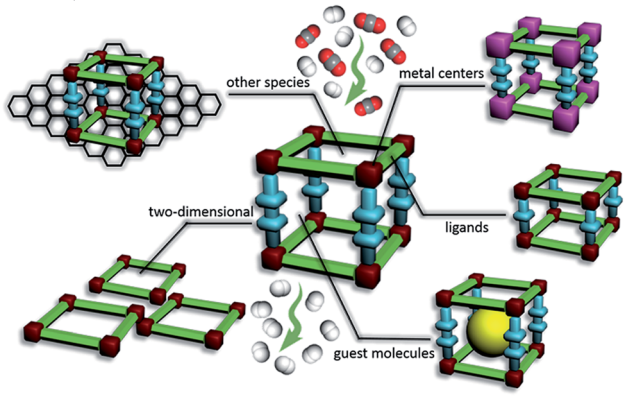

Fig. 2 Strategies for improving the separation performance of membranes based on MOF structures.

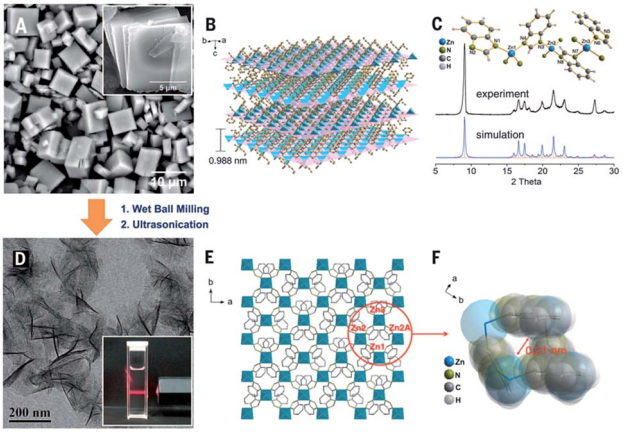

Fig. 3 Top-down fabrication of molecule-sieving nanosheets (MSNs). (A) Scanning electron microscopy (SEM) image of as-synthesized $Zn_2(bim)_4$ crystals. The inset image shows the typical flake-like morphology of the $Zn_2(bim)_4$ crystals. (B) Architecture of the layered MOF precursor. (C) Powder XRD patterns of $Zn_2(bim)_4$. (D) TEM image of $Zn_2(bim)_4$ MSNs. The inset shows the Tyndall effect of a colloidal suspension. (E) Illustration of the grid-like structure of the $Zn_2(bim)_4$ MSN. The Zn coordination polyhedra are depicted in blue, whereas the bim links are represented by sticks. (F) Space-filling representation of a four-membered ring of the $Zn_2(bim)_4$ MSN. (Reprinted with permission from ref. 40. Copyright 2014 Science.)

mode, and modulating the synthesis by using capping agents to facilitate the MOF crystal growth along the 2D directions.[86,87]

The first ultrathin membrane composited with a pure MOF nanosheet for gas separation was reported by Prof. Yang and co-workers.[71] They presented a reliable method for producing stable, size-selective MOF membranes with MOF nanosheets for the separation of H_2 from CO_2. Their approach enabled them to grow MOF membranes showing high selectivity for H_2 over CO_2 while maintaining high permeance. The researchers chose a layered MOF precursor poly[Zn_2(benzimidazole)$_4$] ($Zn_2(bim)_4$), whose bulk structure comprised stacked sheets of Zn(bim) held together through weak van der Waals interactions (Fig. 3a–c). To maintain the structural integrity of the MOF in-plane, a gentle exfoliation process (wet ball-milling with low speed) was carried out to make the bulk MOF into a MOF nanosheet (Fig. 3d). Several solvents were tried in the system, and it turned out that a mixture of methanol and propanol was suitable for stabilization of the layers. In the next step, MOF nanosheets with the same sieving and sorption properties of the bulk MOF phase were made into an ultrathin membrane *via* a hot-drop coating to avoid the order stacking of the nanosheets, which could otherwise result in partial or total blockage of the molecular sieve pores. As we discussed above, an ultrathin membrane with a unique pore size may possess both ideal selectivity and permeance. For this, the $Zn_2(bim)_4$ membrane with a nanometer thickness, due to having MOF cages of 0.21 nm (Fig. 3e and f) and flexibility, resulted in excellent size selectivity for H_2/CO_2 (>200) through the MOF pores, as well as a high permeance (up to 3760 GPU). The most exciting aspect of this work was the elegant extension from fundamental studies of membranes to real-work application testing.[88] The gas separation tests were carried out on this membrane at a challenging condition, culminating in a complex stream study of H_2 gas separation from an equimolar H_2/CO_2 feed containing ~4 mol% steam at 150 °C. The result indicated that the membranes maintained selectivity for H_2 with good thermal stability over 120 h of continuous testing.

Beyond the top-down method, MOF nanosheets can also be obtained by directly adjusting the synthesis system, which may give a high yield. Prof. Gascon *et al.* presented a bottom-up synthesis strategy for copper 1,4-benzenedicarboxylate (CuBDC) MOF lamellae with micrometer lateral dimensions and nanometer thickness involving diffusion-mediated modulation of the MOF growth kinetics. As illustrated in Fig. 4, three kinds of liquids were vertically arranged according to their different densities, composing the synthesis medium as a cocktail. Metal salt $Cu(NO_3)_2$ and BDCA linkers were solved in the top and bottom solvent layers, separated by an intermediate solvent layer. Under static conditions, Cu^{2+} and BDCA ligands diffuse into the spacer segment slowly and form the MOF nanosheet in a highly diluted medium. As the thickness of the sheet in this work is in range of 5–25 nm, the author incorporated the MOF nanosheets into polymer matrices to prepare MMMs. Composites incorporating 2D nanostructures within polymeric matrices have potential as functional components for several techniques, including gas separation, whereby gas molecules with a larger size have to pass a farther way round the nanosheet in the polymer, while smaller gas molecules can directly pass through the lamellae. Furthermore, the 2D filler can reduce the whole thickness of the membrane as well. In this work, the author studied the condition of a nanosheet dispersed in the matrix compared with isotropic crystals *via* tomographic analysis using focused ion beam scanning electron microscopy. MMMs with the filler of CuBDC nanosheets gave an excellent CO_2 separation performance from CO_2/CH_4 gas mixtures as the MOF nanosheet improved the molecular discrimination efficiency and eliminated the unselective permeation pathways.

The study above revealed the great potential of MMMs containing MOFs with lamellar morphologies as fillers. However, a facile and economical way to synthesize lamellar MOFs still remains challenging. In the work reported by Prof. Zhao *et al.*,[47]

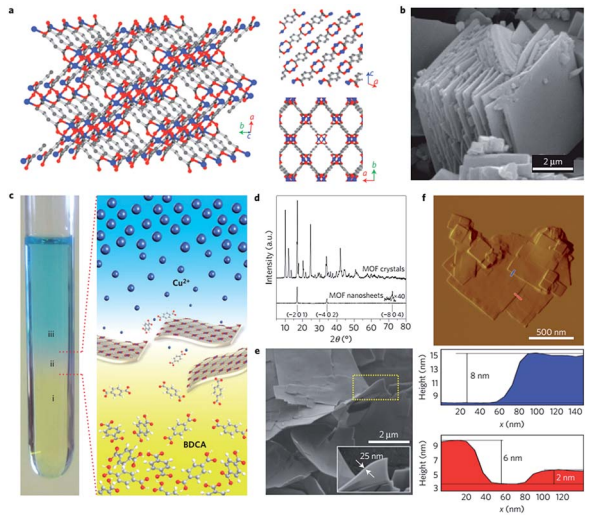

Fig. 4 Synthesis and structure of the metal–organic framework nanostructures. (a) 3D crystalline structure of CuBDC MOF. The insets on the right-hand side show views along the *b* (top) and *c* (bottom) crystallographic axes showing the stacking direction and the pore system, respectively. (b) SEM of bulk-type CuBDC MOF crystals. (c) Image showing the spatial arrangement of different liquid layers during the synthesis of CuBDC MOF nanosheets. Layers labeled as (i, ii, and iii) correspond to a benzene 1,4-dicarboxylic acid (BDCA) solution, the solvent spacer layer, and the solution of Cu^{2+} ions, respectively. (d) X-ray diffraction for the bulk-type and nanosheet CuBDC MOF. (e) and (f) SEM and AFM, respectively, for CuBDC MOF nanosheets synthesized as illustrated in (c). (Reprinted with permission from ref. 46. Copyright 2015 Nature publishing group.)

MOFs $[Cu_2(ndc)_2(dabco)]_n$ (ndc = 1,4-naphthalene dicarboxylate, dabco = 1,4-diazabicyclo[2.2.2]octane)[89] with various morphologies (bulk crystals, nanocubes, and nanosheets) were prepared using a modulated synthetic approach. The MOF is a typical 3D framework composed of a layer structure pillared by dabco, which can be made into nanocubes and nanosheets by adding different capping agents in either of two directions. The MOF nanosheets were obtained by refluxing a metal salt, linkers, and the capping agent pyridine for 24 h in an ethanol solution, giving a good yield. This method to prepare MOF nanosheets is easy to operate and can be facilely scaled up. The author then blended the MOF material with polymer into MMMs and studied the relationship between the filler morphology and membrane performance. Similar to the research above, the lamellar nanosheet can serve as effective CO_2 barriers, thus improving the gas separation performance. MMMs with a MOF nanosheet loading amount of 20 wt% exhibited a H_2 permeability of 6.13 ± 0.03 barrers and a H_2/CO_2 selectivity of 26.7, which exceed the 2008 Robeson upper bound.[16]

MOF nanosheets can also serve as seed crystals to grow a thin MOF membrane, which was successfully achieved in the field of thin zeolite membrane preparation.[90] However, some MOF materials with a suitable pore size and stability are difficult to make into nanosheets, such as the famous ZIF-8. Other 2D materials, such as GO, can be used as templates to get 2D composite nanosheets. Wang *et al.* reported a strategy to fabricate ultrathin and defect-free membranes by the secondary growth of a 2D hybrid MOF/GO seeding layer on various porous substrates.[48] Specifically, hybrid MOF nanosheets were formed by growing MOF nanocrystals on both sides of 2D GO nanosheets, giving a sandwich-like structure (Fig. 5). Hybrid nanosheets were then dispersed on the substrate (AAO or Nylon) by a spin-coating method, resulting in a uniform seeding layer. The contra-diffusion method was used for the second growth process to avoid crystal overgrowth and defects. In this program, the ZIF-8 crystal loading amount and second growth time were studied to obtain the suitable conditions. As a result, the ZIF-8/GO layer with 3 h seed synthesis time and second growth time, respectively, was composed of well-intergrown ZIF nano-grains, and had a thickness of about 100 nm, which made it one of the thinnest ZIF-8 membranes ever reported. The ZIF-8/GO membrane exhibited an ideal separation selectivity of 405 for H_2/C_3H_8 and 7 for CO_2/N_2. This strategy showed great potential for the application of platform technology in the fabrication of ultrathin membranes from various crystalline porous materials.

Fine-tuning of the pore size

In many microporous materials used for membranes, there is a trade-off between permeability and selectivity for gas mixture separation, making it difficult to achieve high separation efficiency for the membrane process. In the first section, we discussed the various approaches to enhance the gas permeance with ideal selectivity by reducing the thickness. On the other hand, to realize molecular sieving, high selectivity can also be achieved by varying the pore size of the solid media. However, it is challenging to generalize this idea to zeolites and carbon molecular sieves (CMSs) because zeolites have a limited number of crystal structures and CMSs have amorphous pore structures. MOFs, however, can form a vast variety of ordered structures, pore sizes, and porosities with functional groups from the different arrangements of metal centers and bridging organic ligands.[91,92] MOFs can be made into effective membranes for gas separation by fine-tuning the pore size using various methods.

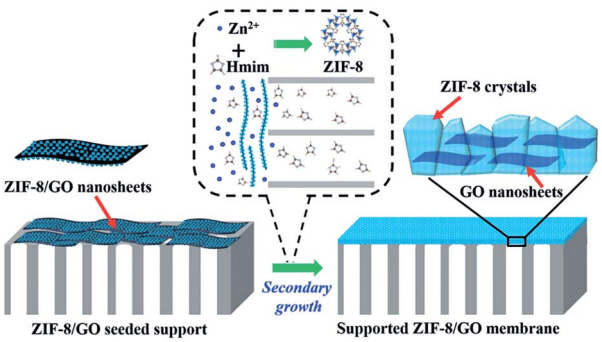

Fig. 5 Schematic of the synthesis process of an ultrathin ZIF-8/GO membrane: coating of flexible ZIF-8/GO nanosheets on a porous support, such as anodic aluminum oxide (AAO), and subsequent secondary growth by the contra-diffusion method. (Reprinted with permission from ref. 48. Copyright 2016 Wiley.)

We will discuss three main paths to adjust the pore size of MOF membranes.

The first and most direct method is by using different ligands to replace a similar one in the original MOF structure to obtain a suitable pore size to fit the target molecules.[93,94] In the work reported by Prof. Caro and Fischer *et al.*, two MOF membranes with similar structures and different pore sizes were prepared by the stepwise deposition of reactants.[49] Two-pillared layered MOFs with the general formula $[Cu_2L_2P]_n$ (L = dicarboxylate linker, P = dabco) were prepared into membranes on a substrate of porous TiO_2 and α-Al_2O_3 disks by a step-by-step, liquid-phase deposition. Membrane 1 was composited with non-polar L = ndc, while, membrane 2 was built by the polar linker L = 2,5-bis(2-methoxyethoxy)-1,4-benzene-dicarboxylate and pillar dabco. Single gas and mixture gases permeability tests were evaluated on both membranes using the Wicke–Kallenbach technique. For the equimolar CO_2/CH_4 mixtures, membrane 2 possessed anti-Knudsen CO_2/CH_4 separation factors in the range of 4–4.5 as polar ligands increase the framework affinity to CO_2 compared with CH_4. In contrast, the separation with membrane 1 was found to be Knudsen-like. A much lower pure SF_6 permeance was obtained on membrane 2 compared with membrane 1, due to the smaller pore size (3.5–4 Å) of membrane 2. As the two oriented apertures could be adjusted and as several functional groups are available, this $[M_2L_2P]$ family is suited for such a systematic study of the pore size and adsorption effect on the gas separation of MOF membranes.[95] The stepwise deposition method can be optimized to improve the separation factor.

In another work from Prof. Qiu's group, two nickel screen-supported MOF membranes with pillars of different lengths were successfully synthesized by a secondary growth method. As shown in Fig. 6, pillared layered MOFs of Ni_2(L-asp)$_2$P were chosen. In this case, two different pillared ligands, namely 4,4-bipyridine and pyrazine, were used to adjust the pore size of the membrane material. For the membrane with the longer pillar, an ideal H_2 permeance of 1.82×10^{-6} mol m^{-2} s^{-1} Pa^{-1} and a separation factor higher than the Knudsen diffusion coefficient were obtained due to the large pore size and selective adsorption of gas on the MOF. The ultra-microporous JUC-150 membrane with the shorter pyrazine ligands showed preferential permeation for H_2 over the other gas molecules through its size-sieving effect, leading to high selectivity factors of 26.3, 17.1, and 38.7 for H_2/CH_4, H_2/N_2, and H_2/CO_2, respectively. This study successfully proved that the membrane possessed tunable pore sizes and designable pore surfaces, where also the uniform pore distribution of the MOF membranes make them very promising for gas separation.

Moreover, partial replacement of the ligands can adjust the pore size effectively. Prof. Nair *et al.* carried out several works on this point.[96–98] In their recent work, they prepared a series of mixed-linker ZIF-8-90 frameworks. ZIF-8 and ZIF-90 have the same SOD topology, whereas they are composited of different ligands. The adjustment of the ratio of mixed ligands brought about the tunability of the effective pore size as well as the ratio of polar to non-polar functional groups in the framework, which led to the continuous tuning of their molecular sieving and adsorption behavior.[97] Micro-Raman composition analysis was carried out on the individual ZIF-8-90 crystals to prove the hybrid nature and high uniformity of the mixed-linker materials. As shown in Fig. 7, different adsorption and diffusion behavior based on the tunable molecular sieving were observed on continuous tuning of the pore size. The *n*-butane and i-butane diffusivities and the *n*-butane/i-butane diffusion selectivity could be continuously tuned over several orders of magnitude. This study on the tunable adsorption and diffusion properties in ZIF-8-90 materials plays a heuristic and guiding role in research on membrane separation using hybridized ligands to adjust pore size.

The second main approach to adjusting the pore size involves exchanging the other part of the MOF, *i.e.*, the metal center. For MOF materials, the single crystal to single crystal (SCSC) transformation technique is usually used to obtain a more stable crystal framework for MOFs, where it is difficult to synthesize or fine tune the pore size.[99–102] In the work of Prof. Zhang, they involved this transforming strategy to the field of MOF membrane fabrication based on multivalent cation substitution.[51] They communicated their key discovery with two examples, one was the transformation of CuBTC to MIL-100, which had the advantages of easy preparation and material

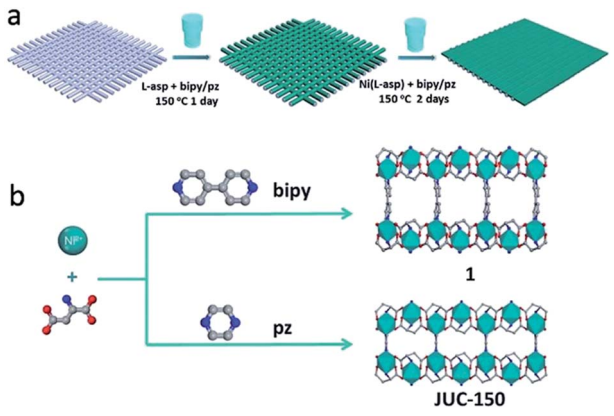

Fig. 6 (a) Schematic of the preparation of Ni_2(L-asp)$_2$P membranes on nickel screens. (b) Schematic of compound 1 and its JUC-150 structure. (Reprinted with permission from ref. 50. Copyright 2014 RSC.)

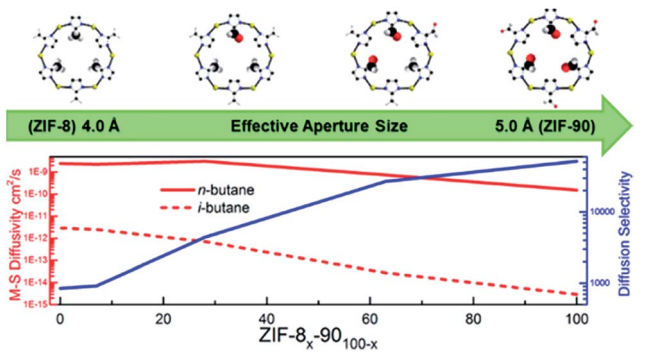

Fig. 7 Schematic of the continuous tuning of the molecular sieving and adsorption behavior in mixed-linker ZIF-8-90 frameworks. (Reprinted with permission from ref. 97. Copyright 2015 American Chemical Society.)

stability, the other involved the transformation of CuBTC membrane to the CuBTC/MIL-100 membrane, which provided a facile route to design promising candidate MOF membranes for molecular sieving. For the case of CuBTC/MIL-100 (Fig. 8), after transformation, the void interfaces could be eliminated, the gas channel could be reduced, and the gas selectivities of the transformed membrane were increased. Because of the tailorable pore sizes of MOF materials and the diversity in membrane synthesis, they envisaged there would be some optimal MOFs and proper preparation conditions, where the membranes with a lower thickness and better separation performance could be achieved by transformation in the future.

Based on the same structure and different metal centers, Prof. Jeong *et al.* reported well inter-grown membranes of ZIF-67 by heteroepitaxially growing ZIF-67 on ZIF-8 seed layers.[52] As a tertiary growth of ZIF-8 layers was applied to heteroepitaxially grown ZIF-67 membranes, the membranes exhibited unprecedentedly high propylene/propane separation factors of ~200, possibly due to the enhanced grain boundary structure, as illustrated in Fig. 9. While the crystallographically determined pore apertures showed negligible difference between ZIF-8 and ZIF-67, the IR band corresponding to the metal–nitrogen stretching frequency in ZIF-67 (ν_{Co-N}) was blue-shifted as compared to the one in ZIF-8 (ν_{Zn-N}). This blue-shift implied that Co–N bonds were more rigid than Zn–N bonds. Considering the fact that the effective pore aperture of ZIFs depends on

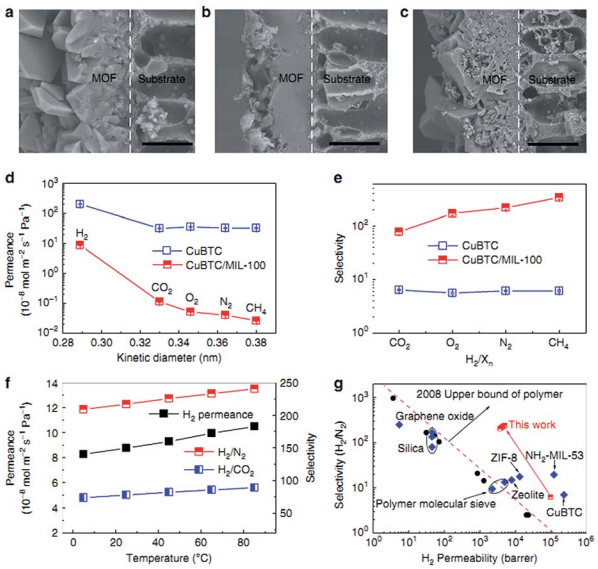

Fig. 8 Transformations of the CuBTC membrane and their performance. (a–c) SEM images of the original CuBTC membrane, the transformed CuBTC/MIL-100 membrane, and the transformed CuBTC/MIL-100 membrane after purification, respectively. Scale bar, 20 mm. (d and e) Gas permeance and selectivities of the CuBTC and CuBTC/MIL-100 membranes. All the average permeation results with standard deviation were calculated from three measurement data. (f) Effect of temperature on H_2 permeance and H_2/CO_2 and H_2/N_2 selectivity for the CuBTC/MIL-100 membrane. (g) Comparison of the CuBTC/MIL-100 membrane with other kinds of membranes for the H_2/N_2 system. The red dotted line is the Robeson's upper-bound reported in 2008. (Reprinted with permission from ref. 51. Copyright 2016 Nature publishing group.)

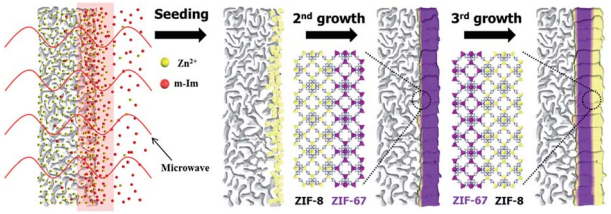

Fig. 9 Schematic of the membrane synthesis *via* heteroepitaxial growth. (Reprinted with permission from ref. 52. Copyright 2015 American Chemical Society.)

the magnitude of the ligand flipping motion, it is not unreasonable to surmise that the more rigid the metal–nitrogen connectivity is, the less the degree of the ligand flipping motion is. This restricted motion might lead to the slightly smaller effective pore aperture of ZIF-67 and consequently improved separation factors. The remarkable propylene/propane separation performances prove that different metal centers can affect the pore size of MOFs, leading to an improvement in gas separation selectivity.

The third method for changing the pore environment is by loading some guest molecules into the channels of the MOFs through adjusting the pore size and converting the interaction between the gas molecules and host MOF framework. This strategy was originally used in zeolite membranes for fine-tuning the pore size of the LTA-type membrane by ion-exchange.[103,104] As for the MOF membrane, this strategy can also be widely used due to the abundant functional groups of MOF materials. Caro *et al.* developed a covalent post-functionalization strategy to modify the ZIF-90 membrane with ethylenediamine to enhance its hydrogen selectivity.[26] The post-functionalization strategy was not only helpful in eliminating intercrystalline defects but could also constrict the pore aperture, giving improved molecular sieving for better gas separation. In another study, ZIF-90 membrane was modified by 3-aminopropyltriethoxysilane (APTES), which was also used as the linker between the membrane and substrate.[53] Because of both pore size narrowing and sealing of the invisible intercrystalline defects by APTES, the separation performances for a CO_2/CH_4 mixture on the obtained membrane were remarkably enhanced, achieving a CO_2 permeance of 1.26 × 10^{-8} mol m^{-2} s^{-1} Pa^{-1} and a CO_2/CH_4 selectivity of 4.7. The amine-modification method was also applied to Mg–MOF-74,[54] which was a promising material for CO_2 capture.[105] The selectivity of H_2/CO_2 was significantly improved from 10.5 to 28 as the modified amino group narrowed the effective pore size and strengthened the interaction between the CO_2 and the framework. All these three research studies proved that guest molecule post-modification is an effective method to enhance the gas separation performance by tuning the pore size.

In the cases above, guest molecules were assembled in the pores of MOF frameworks to improve their gas separation properties by post-functional processes, which usually require steps additional to the synthesis. In a recent work, tailoring of the pore size was achieve by an *in situ* synthesis, while keeping the original guest molecules in the structure.[55] Based on the

parent MOF $[Ni_2(L\text{-asp})_2(bipy)]$, it was observed that the bpe (1,2-bis(4-pyridyl)ethylene) pillar linker had the same connectivity as the bipy ligand in constructing the $[Ni_2(L\text{-asp})_2(bpe)]\cdot(G)$ framework (G = guest), which confined the excess bpe ligand in the channels. The guest molecules were encapsulated in the pores during the membrane fabrication step with better dispersion. The bpe molecules uniformly distributed in the channels not only reduce the window size, but also enhance the interaction between the MOF framework and the CO_2 gas molecules, which makes the membrane suitable for H_2/CO_2 separation. The membrane presented a high permeance for H_2 (1.0×10^{-6} mol m^{-2} s^{-1} Pa^{-1}) and provided desired selectivity (24.3) for binary gas mixtures of H_2/CO_2.

Similar to the classic LTA-type zeolite, ZIF-8 is a kind of cage-type MOF with a SOD topology, where the cage and window size are 1.12 nm and 0.34 nm, respectively. As shown in Fig. 10, Yang's group demonstrated that ionic liquids (ILs), at room temperature, can be used as cavity occupants to fine tune the effective cage size of ZIF-8.[41] By adding an ionic liquid into the ZIF-8 synthesis system, IL@ZIF-8 with a suitable microenvironment for CO_2/N_2 selective adsorption was obtained. The ideal adsorption selectivity of CO_2/N_2 on IL@ZIF-8 was enhanced from 19 to 100 compared with the original ZIF-8. Furthermore, MMMs based on the IL@ZIF-8 possessed remarkable combinations of permeability and selectivity that transcended the upper bound of polymer membranes for CO_2/N_2 and CO_2/CH_4 separation.

MOF membranes combined with other species

Generally, MOF synthesis involves coordination bonding between metal centers and organic ligands. Therefore, a particularly favorable case is encountered when the substrate is made from the same metal source of MOF. This scenario can enhance the interfacial bonding between the MOFs and substrates.[106] Qiu's group reported an HKUST-1 membrane grown on a copper net substrate by means of a 'twin copper source' technique.[33] The copper net was first oxidized to copper oxide at 100 °C, and was then converted to a HKUST-1 membrane in the HKUST-1 mother solution. Furthermore, the same group developed a simpler 'single metal source' method later to facilely prepare a homochiral MOF membrane on the nickel net, which played a dual role in the synthesis process as the only nickel source added to the reaction system and as a substrate supporting the membrane.[107] Since the nickel net was the only metal source in the reaction system, the growth process stops once a layer of crystal film is formed, making the final membrane thinner and continuous. This provides MOF-based membrane separation with a great improvement.

Sometimes, due to the composition, morphology, or reactivity, the substrates are not suitable to act as direct precursors, and need to be first covered by some "fertile soil" for development of the MOF membranes. Prof. Liu and Prof. Caro *et al.* developed a urea hydrolysis method to *in situ* prepare asymmetric ZnAl-CO_3 layered double hydroxide (LDH) buffer layers with various stable equilibrium morphologies on porous Al_2O_3 substrates.[56] The γ-Al_2O_3 phase on the substrate served as the Al^{3+} source for the homogeneous nucleation and for the subsequent growth of the LDH buffer layer. As shown in Fig. 11, because of the metal–imidazole interaction between ZnAl-CO_3 LDHs and ZIFs, Zn-based ZIFs membrane, such as ZIF-8, ZIF-7, and ZIF-90, were successfully prepared on the LDH-covered substrate, giving a new concept for substrate modification.

In the work of Prof. Drobek *et al.*, to obtain a high-quality ZIF-8 membrane, the atomic layer deposition (ALD) of ZnO thin films on the grains of a macroporous ceramic support was carried out.[57] Compared to other deposition techniques, ALD is particularly well adapted for both controlling the thickness of the deposited layers and for uniformly covering the grains of the support surface and bulk. By optimizing the experiment conditions, a suitable ZnO thickness and transforming temperature were found to be key factors to prepare good quality ZIF-8 membranes. This eco-friendly synthesis method may be used to deposit different oxides materials on various kinds of substrates and to convert them to other MOFs.

As mentioned, some other species may act as the precursor for the MOF membrane and may then be transformed to MOF

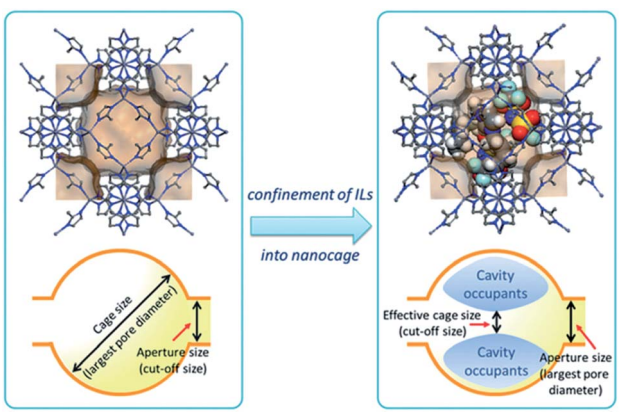

Fig. 10 Schematic of the cavity-occupying concept for tailoring the molecular sieving properties of ZIF-8 by the incorporation of room temperature ionic liquids (RTILs). The cut-off size shifts from the aperture size of the six-membered ring to the reduced effective cage size by the confinement of ILs in a ZIF-8's SOD cage. (Reprinted with permission from ref. 41. Copyright 2015 Wiley.)

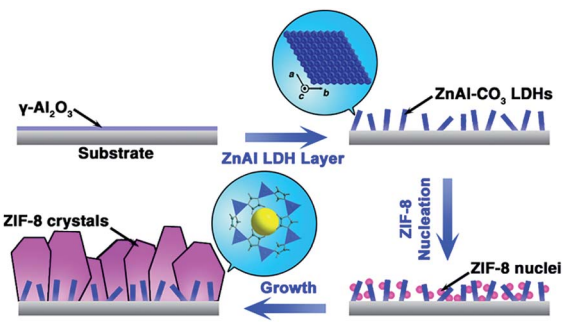

Fig. 11 Schematic of the *in situ* solvothermal growth of the ZIF-8 membrane on a ZnAl-LDH buffer layer-modified γ-Al_2O_3 substrate. (Reprinted with permission from ref. 56. Copyright 2014 American Chemical Society.)

materials. Besides the precursor, other species can also be added into the MOF membrane synthesis system to form composite materials and to be part of the membrane.[58,109] Prof. Peng *et al.* demonstrated the complete conversion of a copper hydroxide nanostrand (CHN) free-standing thin film into a pure phase HKUST-1 free-standing membrane in a water–ethanol solution at room temperature.[108] The morphology of the HKUST-1 crystals could be easily tuned from truncated cubes to cuboctahedrons, depending on the reaction time, without any other additive modulators. Then, the same author reported that diverse functional components, including small ions, micrometer-sized particles, inorganic nanoparticles, and bioactive proteins, can be encapsulated in MOF thin films *via* the above-mentioned room temperature conversion technique. As illustrated in Fig. 12, CHNs and doping species were mixed together and filtrated to the porous substrate, and then reacted with the ligand of BTC to form component-encapsulated MOF composite thin films. This strategy can be used to involve 2D barriers, such as GO, in the membrane to improve the gas separation performance.

Defects between the crystals are a major issue and can reduce the selectivity of the MOF membrane. Other species can also be used as "repair agents" to fix these defects of MOF membranes. Polymers have been used as the sealant for the LTA membrane by a "float casting" strategy.[110] For the MOF membrane, Prof. Huang *et al.* deposited GO on a semi-continuous ZIF-8 layer (Fig. 13), and then prepared a novel bicontinuous ZIF-8@GO membrane. The molecule-sieving effect was enhanced because the GO layer fixed the gaps between the ZIF-8 crystals, such that the gas molecules have to go through the small window of ZIF-8. The mixture separation factors for H_2/CO_2, H_2/N_2, H_2/CH_4, and H_2/C_3H_8 on the ZIF-8@GO membrane were 14.9, 90.5, 139.1, and 3816.6, respectively, with H_2 permeances of nearly 1.3×10^{-7} mol m^{-2} s^{-1} Pa^{-1}, which are promising for hydrogen separation and purification by molecular sieving. On the contrary, MOF materials can also be used to fix the gaps in GO membranes. Prof. Zhao's group developed a novel approach to narrow the non-selective

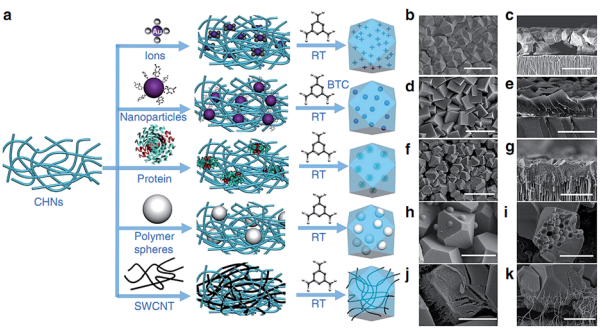

Fig. 12 Schematic of the synthesis process and SEM images. (a) Scheme of the synthesis process of functional components encapsulated HKUST-1 composite thin films through a pre-confined technique by using CHNs; (b and c) $[AuCl_4]^-$ ions, (d and e) 20 nm Au nanoparticles (20 nm), (f and g) ferritin, (h and i) 620 nm polymer sphere and (j and k) single-walled carbon nanotubes (SWCNTs), encapsulated HKUST-1 composite thin films, respectively. (Reprinted with permission from ref. 108. Copyright 2014 Nature publishing group.)

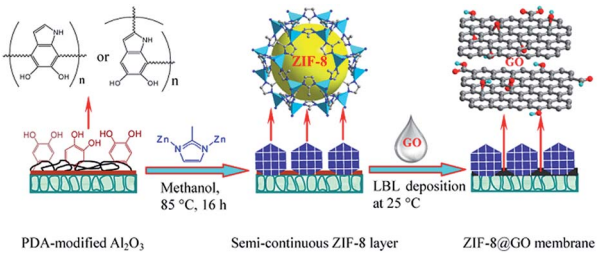

Fig. 13 Schematic of preparation of bicontinuous ZIF-8@GO membranes through the layer-by-layer deposition of graphene oxide on the semicontinuous ZIF-8 layer, which was synthesized on a polydopamine-modified alumina disk. (Reprinted with permission from ref. 59. Copyright 2014 American Chemical Society.)

pores of GO membranes by the intergrowth of ZIF-8 crystals. The obtained membranes exhibited excellent H_2 separation performance.[111]

In a recent work reported by Prof. Qiu *et al.*, they initially demonstrated that MOF could be grown on a covalent-organic framework (COF) membrane to fabricate COF–MOF composite membranes.[42] The resultant COF–MOF composite membranes showed higher separation selectivity of H_2/CO_2 gas mixtures than the individual COF and MOF membranes. The TEM characterization results in Fig. 14 show that there were two

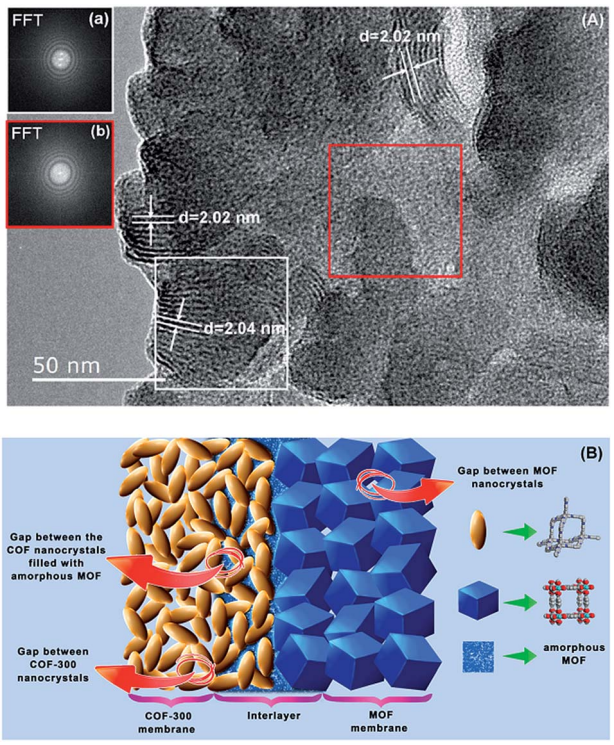

Fig. 14 (A) TEM image and FFT analysis (shown in insets a and b) of the [COF-300]–[Zn_2(bdc)$_2$(dabco)] composite membrane. Inset (a) is the FFT of the white marked area, and inset (b) is the FFT of the red marked area. (B) Schematic of the interlayer formed by amorphous MOF, which has a similar pore size as a crystalline MOF, occupying the gaps between the COF nanocrystals and the interface between the COF and MOF crystalline layers. (Reprinted with permission from ref. 42. Copyright 2016 American Chemical Society.)

parts, a crystalline and an amorphous part, in the composite layer. The crystalline part could be recognized by the lattice fringes and roundish morphology of the COF-300 nanocrystallites, while the amorphous part was filling the space between the shaped crystalline particles. The EDS spectrum of the amorphous part revealed the presence of zinc, which highlighted that the amorphous phase that filled the gaps between COF crystals was of a MOF-type. The COF nanocrystallites were integrated in the amorphous matrix, and no interface between the two phases could be observed. The amorphous MOF possessed a similar pore size to that of the crystalline MOF, but lacked the long-range order. This amorphous MOF layer in the COF–MOF composite membranes was beneficial for membrane selectivity and permeance, since it sealed the space between COF crystals and maintained a similar pore size to that of the individual COF and MOF layers. This work suggested that the MOF membrane could be combined with other porous materials to form a sandwich-like multilayer membrane with enhanced gas separation performance.

Challenges for MOF membranes

Over the last decade, we have witnessed the fast growth of MOF membranes due to their potential application in high-quality performance gas separation.[34,38,112–117] However, MOF membranes still allow prospects for further practical application in industry, but the development of truly functional membranes will probably take more time. Simpler, cheaper, and high-yield synthesis methods are expected to lead to the preparation of MOF membranes on the large scale. Additionally, MOF membranes with enhanced stability are required for practical separation conditions, such as high temperature and pressure. In this section, we discuss the recent research, mainly focusing on the challenges remaining for MOF membranes.

Scale-up of MOF membrane

MOFs that are identified to be good membranes on the lab scale must be scaled up and tested in practical applications. Similar to zeolites, scalability is expected to be the main barrier before commercialization of the MOF membranes can occur.[116] (1) The high cost of support materials and organic ligands, (2) the hydrothermal and solvothermal synthesis process, and (3) large-area membrane quality are three main issues for the scale-up of MOF membranes. It is certain that a shorter term industrial application of MOFs in membranes will occur in MMMs, where MOFs are used as filler particles in small amounts in polymers. MMMs comprising both polymers and inorganic components offer a good compromise to address the limitations of either of the individual components.[118–121] Research on MMMs begun in the late 1980s, when they were first based on the filler of zeolite. However, the poor compatibility of zeolite and polymer led to a gap or dense phase between the two species, which degrades the performance of the obtained composite membrane. MOFs, on the other hand, are composited of a metal center and organic linkers, which can have a strong interaction with the polymer matrix. MOF-based MMMs have received increasing attention, which has led to rapidly expanding literature reports.[67,122–128] The research of MMMs was mainly focused on membranes prepared by different fillers and polymers with improved property. Most of the membrane areas were limited to the lab scale, with no prominence attached to the advantages of the introduction of polymers. Much less efforts have been made to advance MMMs into asymmetric hollow fibers,[121,128,129] which are the most practical membrane geometries in terms of membrane packing efficiency.[130]

In Prof. Koros group's work, they successfully formed dual-layer ZIF-8/6FDA-DAM mixed-matrix hollow fiber membranes with ZIF-8 nanoparticle loading up to 30 wt% using the conventional dry-jet/wet-quench fiber-spinning technique.[60] In that work, the challenges to develop scalable MMMs and desirable characteristics of dual-layer mixed-matrix hollow fiber membranes were discussed in detail (Fig. 15). Aimed at these characteristics, they successfully fabricated highly scalable, high-loading ZIF-8/6FDA-DAM mixed-matrix hollow fiber membranes on the basis of the successfully developed ZIF-8/6FDA-DAM mixed-matrix dense films and neat 6FDA-DAM hollow fibers. To achieve a high loading of ZIF-8 and to avoid defects, a post-treatment of a core layer of 6FDA-DAM by coating with polydimethylsiloxane (PDMS) and/or polyaramid is a critical step to seal fiber skin defects. The hollow fiber C_3H_6/C_3H_8 selectivity increased with the increasing ZIF-8 loading up to 30 wt%, consistent with the previously reported dense film permeation data. Therefore, this represents great progress in the research area of advanced MMMs, especially in the scale-up field.

MMMs have aroused much interest owing to its composition of polymers, which allows relative easy processing into morphologies, such as hollow fibers.[131] As previously discussed, for the molecular sieving membranes, one challenge is the lack of an easily scalable, reliable, and benign fabrication process.[132–134] Zeolite membranes are further hampered by the requirement for hydrothermal synthesis on high-cost support materials. MOFs have been used to grow crystalline membranes on disk and tubular substrates through techniques similar to those developed for zeolite membranes. Growing large-area MOF membranes on the surface of hollow fibers is a challenging and important topic for the practical application of MOF membrane separation.

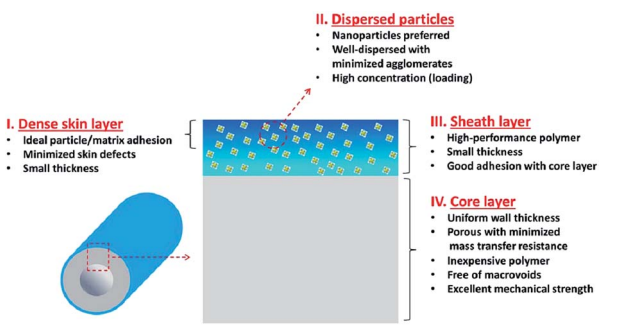

Fig. 15 Schematic and desirable characteristics of dual-layer mixed-matrix hollow fiber membranes. (Reprinted with permission from ref. 60. Copyright 2014 American Chemical Society.)

A series of pioneer works were done by Prof. Nair to prepare ZIFs membrane on the substrates of hollow fibers. A ZIF-90 membrane was fabricated on the outside of a porous polymeric poly(amide-imide) hollow fiber by a seed-secondary growth method.[135] Growing MOFs on the inner surfaces of hollow fibers has several advantages, including the ability to be bundled in close proximity while avoiding membrane–membrane contact points and interfaces that lead to defects during synthesis. The synthesis of selective membranes in microscopic confined spaces confronts researchers with plenty of challenges such as reactant availability and transport, positional control of the membrane, and scalability. In the work reported by the same group, interfacial microfluidic membrane-processing (IMMP) methodology was used to grow ZIF-8 membrane on the inside of Torlon hollow fibers.[43] As shown in Fig. 16, IMMP combined three key concepts: (i) *in situ* ZIF-8 film synthesis in the membrane module; (ii) a two-solvent interfacial approach that could be tuned to achieve positional control over the membrane formation and (iii) the controlled supply, replenishment, and recycling of reactants at microfluidic conditions in the hollow fiber bore. An interesting detail in this work was that a lumen-capping step was carried out to seal the end of the hollow fiber with PDMS, avoiding membrane bypass to achieve a better molecule-sieving effect. The membrane-processing approach in this work is a notable step toward realizing scalable molecular sieving MOF membranes.

Prof. Coronas also developed a ZIF membrane preparation based on microfluidics.[61] As can be seen in the scheme of the experimental setup shown in Fig. 17, both the metal salt and ligand solution were pumped through the fiber lumen to obtain continuous and thin layers of ZIF-7 and ZIF-8 on the inner face of a hollow fiber. Compared with Nair's work, the flowing of both reagents gave rise to additional reactants and solvent savings. The same group also expanded this method to prepare a ZIF-93 membrane on the support of P84 co-polyimide HF.[62] Because of the molecule-sieving mechanism, the obtained membrane possessed high selectivity of 59.7 and 16.9 for the separation of H_2/CH_4 and CO_2/CH_4.

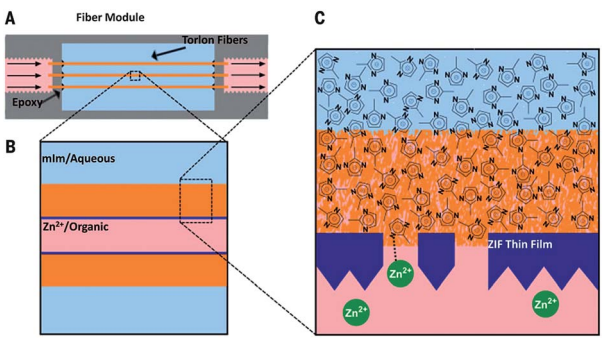

Fig. 16 Schematic depicting the IMMP approach for MOF membranes in hollow fibers. (A) Side view of a series of fibers mounted in the IMMP reactor. (B) The Zn^{2+} ions are supplied in a 1-octanol solution flowing through the bore of the fiber, whereas the methylimidazole linkers are supplied on the outer side of the fiber in an aqueous solution. (C) Magnified view of the fiber support during the synthesis. The membrane forms on the inner surface of the fiber by reaction of the two precursors to form a ZIF-8 layer. (Reprinted with permission from ref. 43. Copyright 2014 Science.)

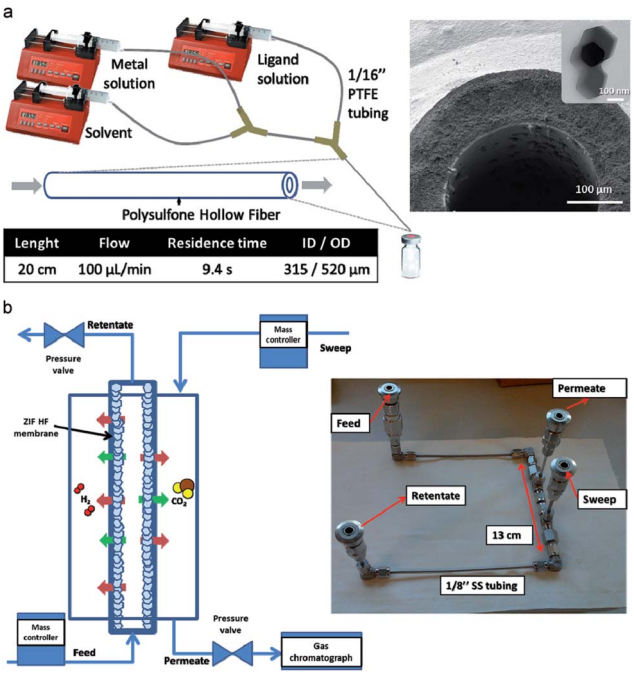

Fig. 17 (a) Microfluidic experimental setup for membrane synthesis, ZIF-8 membrane cross-section, and crystals collected at the exit during the synthesis are shown. (b) Gas plant scheme and experimental stainless-steel module used for HF membrane permeation tests. A 13 cm long hollow fiber was sealed with epoxy resin, where a gas mixture to be separated is fed inside the fiber. The permeate stream is swept cross-current. (Reprinted with permission from ref. 61. Copyright 2015 Elsevier.)

Besides microfluidic-based membrane preparation, several other techniques could potentially be scale-up methods for MOF membrane fabrication. In a work reported by Prof. Qiu and his co-authors, an electrospinning technique was introduced into the synthesis of supported microporous membranes.[63] This approach is suitable for various substrates, especially tubes, with the possibility of large-area processing. The thickness of the seed layer could be precisely controlled to obtain a continuous and uniform seed coating on the support surface. At first, defect-free ZIF-8 membranes were successfully synthesized. Then, they successfully synthesized several kinds of microporous materials into high-quality membranes and films on different-shaped supports by this method,[136] such as zeolite NaA and beta membranes on a porous Al_2O_3 tube, zeolite NaY membrane on a stainless-steel net, and a MOF $Eu(BTC)(H_2O)\cdot DMF$ film on a porous silica disc.

Prof. Kim reported their work on synthesizing supported ZIF-7 films and membranes at ambient pressure using a simple electrospray deposition technique.[64] Compared with Qiu's work, no polymer was added to the precursor solution, which only contained metal ions, ligands, sodium formate, and solvent. During the process of the precursor drop traveling to, landing on, and spreading on the substrate, the solvent was evaporated to induce reactant nucleation and crystallization to form

continuous membranes. The deposition temperature, precursor flow rate, and applied voltage to the precursor solution were important variables to obtain a good quality membrane. This facile method has a potential for scalability. The easy control of the membrane thickness is another attractive point of this method, which can give a thinner membrane and high gas permeance.

Several other techniques for MOF film preparation have been reported recently that may be promising for the large-scale fabrication of separation membranes. In the previous works of Prof. Wöll and Prof. Fischer, liquid-phase epitaxy (LPE) methods have been used to prepare thin MOF films on modified substrates.[35,138,139] Controlling the thickness, orientation, interpenetration, and heteroepitaxy can be achieved by this LPE method.[140–142] In the research reported by Prof. Eddaoudi's group, a defect-free ZIF-8 membrane was prepared on a porous substrate by the LPE method, and the gas separation performance was evaluated by the time-lag technique.[65] The ultrathin (0.5–1 μm) membrane was obtained by cycles of immersing in metal ion and ligand solutions, and a solvent washing process was carried out in the interval of the two solutions to remove excess raw material. In a further work, an adaption of the LPE approach was applied to prepare highly oriented/polycrystalline MOF thin films.[68] As shown in Fig. 18, spin-coating technology was introduced to the LPE process, which made it more effective in terms of a short time and low raw material consumption compared with the conventional LPE process. This method was extended to various MOFs with a 2D or 3D structure and different substrates. The universality, ease of operation, and cost-effective nature make this technique promising for the practical preparation of MOF thin films and membranes. In another work reported by Heinke, a step-by-step spray method was employed to coat a MOF membrane on the substrate.[66] The thickness of the membrane can be controlled by the cycle number of spraying and this method is suitable to scale-up membrane fabrication.

Tradition MOF synthesis is carried out under solvothermal conditions, which is difficult to apply to large-area MOF membrane preparation. Wang *et al.* presented a solvent- and

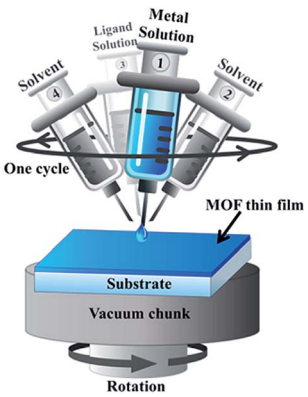

Fig. 18 Schematic representation of the setup employed for the fabrication of MOF thin films using the LPE approach adapted to the spin-coating method. (Reprinted with permission from ref. 137. Copyright 2016 RSC.)

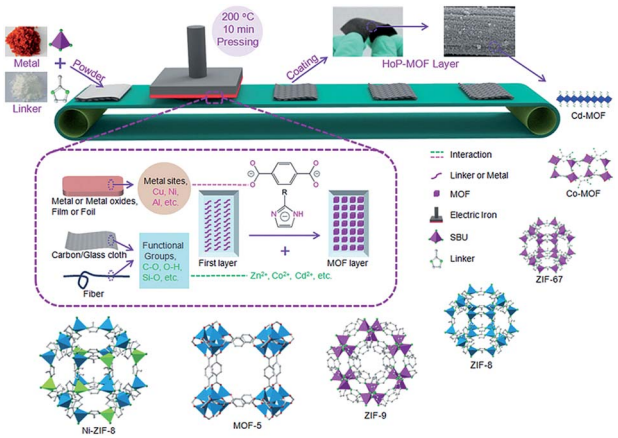

Fig. 19 Schematic of the hot-pressing method for MOF coating. (Reprinted with permission from ref. 143. Copyright 2015 Wiley.)

binder-free approach for producing stable MOF coatings by a unique hot-pressing (HoP) method.[143] The mixture of metal salts and ligands can rapidly react with the surface functional groups or metal sites on the surface of the substrates and then form the MOF layer under applied temperature and pressure simultaneously (Fig. 19). This strategy was proven to be applicable to various MOFs and flexible substrates. A multilayer composite membrane can also be obtained by layer-by-layer pressing. In their follow-up work, this HoP method was scaled up in the form of roll-to-roll production for the mass production of MOF-based filters, which possessed effective particulate matter removal properties for air filtration applications.[144] However, the issues of crystal intergrowth and quality should be addressed for the materials to be used as gas separation membranes.

It will be easy to scale up if the MOF membrane can be polymerized from a monomer like a polymer. This is a fast and facile way to covalently link MOF crystals by flexible polymer chains in an ordered fashion, namely *via* postsynthetic polymerization (PSP). In this way, MOFs that bear polymerizable functional groups can copolymerize with organic monomers to achieve elasticity and processability. However, conventional polymerization methods may inevitably destroy the structures of some MOFs under harsh polymerization conditions or entrap undesirable solvents. In another work reported by Prof. Wang and co-authors, modified UiO-66-NH_2 nanoparticles were copolymerized with acrylate monomers by UV light under solvent-free and mild conditions to form flexible and crack-free membranes for the separation of Cr(VI) ions from water.[145] The advantages of the photoinduced postsynthetic polymerization approach, including its universality and ease of fabrication, may highlight a new direction for the scale-up of MOF membranes with flexibility. The introduction of a polymer monomer may lead to a wider dispersion of pore sizes, thus weakening the molecule-sieving effect of MOFs, which should be considered when applied to the gas separation.

Improved stability of MOF membranes

For most MOFs, one of the major drawbacks is their poor (thermal or chemical) stability, which counts against their

practical applications.[44,146,147] The development of novel stable MOF structures and methods to enhance MOF stability are important research topics, which are critical for the gas separation process on MOF membranes. To date, only a few MOFs have been reported to possess satisfactory hydrothermal stability, *e.g.*, the ZIF family,[93] MIL (Matérial Institut Lavoisier) analogs,[148] and some zirconium- and pyrazolate-based MOFs.[149–151] Otherwise, post-enhancement of hydrothermal stability of the already existing MOF materials is also an attractive option and has become one of the most active research domains nowadays.[44,152,153] The post-enhancement methods, however, need to meet the requirements of keeping the porosity of the parent MOFs after the modification or reinforcement.

ZIF-8 is currently one of the most stable MOFs. Prof. Lin's work demonstrated that the gas permeance on the ZIF-8 membrane for H_2, He, N_2, and SF_6 is hardly changed during days of storage in the lab.[67] The propylene and propane permeance did not change either during 27 days of off-stream storage. Fig. 20 shows the permeation and separation performance of a C_3H_6/C_3H_8 mixture of a ZIF-8 membrane as a function of the off-stream storage time (for 35 days) and on-stream time (for 5 days). The ZIF-8 membrane exhibited constant permeance and selectivity for C_3H_6/C_3H_8 during the entire period of the off-stream and on-stream tests. This work showed that ZIF-8 membranes are extremely stable under both off-stream storage and on-stream C_3H_6/C_3H_8 separation conditions. The excellent stability and ideal separation performance make the ZIF-8 membrane very attractive for propylene/propane separation in industrial applications.

For another kind of famous stable MOF, continuous zirconium(IV)-based MOFs (Zr-MOFs) have also been prepared into membranes. The UiO-66 membranes were fabricated on alumina hollow fibers using an *in situ* solvothermal synthesis method.[154] The water amount in the synthesis solution was a key point to obtain a high-quality inter-grown UIO-66 membrane. Single-gas permeation and ion rejection tests were carried out to confirm the membrane integrity and functionality. The membranes exhibited chemical stability during ion removal from a wide range of saline solutions up to 170 h. Although the pore size of UIO-66 is too large for separating light gas mixtures, stable MOFs based on Zr with a wide range of pore sizes and various functional groups have been reported in the last few years. Furthermore, post-modification and ligand exchange can also be carried out to adjust the pore size of Zr-MOF.

Another effective method to solve the stability problem is to reverse the surface polarity of MOFs from hydrophilicity to hydrophobicity. In the work reported by Prof. Yu's group, hydrophobic PDMS was deposed facilely on the surface of MOF materials.[153] This method was applied to several classic MOFs and the modified materials possessed better moisture or water resistance compared with the pristine MOFs (Fig. 21), and also maintained the original porosity and surface areas. Such a coating process can expand the application of MOF membranes for gas separation in humid conditions. In a recently reported work, this work has been used to switch the surface wettability of a MOF-coated mesh for oil/water separation.[155]

To enhance the stability of ZIFs under hydrothermal conditions, a partial ligand exchange process, referred to as a shell-ligand-exchange-reaction (SLER), was carried out by Li and Yang.[44] As shown in the Fig. 22, 2-MIM ligands in the ZIF-8 crystal outer layer were replaced by 5,6-dimethylbenzimidazole (DMBIM), which made the surface of the crystals hydrophobic. Besides ZIF-8, the SLER methodology was also successfully applied to stabilize other types of ZIFs, such as ZIF-7 and ZIF-93. Same as Yu's work, after the SLER process, the obtained ZIF materials kept the original porosity and had an improved stability under hydrothermal tests. Compared with Yu's work, the shell ligand exchange may possess a more stable surface layer, while causing a complex process.

As discussed in the last section, MOFs-based MMMs can not only possess the easy processing property of polymers but can also fix the inter-crystal defects of polycrystalline MOF membranes to maintain the separation stability of the membrane. Furthermore, MOF fillers can help polymers overcome the issue of plasticization conversely. In the study of Prof. Long, Co_2(dobdc) and Ni_2(dobdc) nanocrystals were combined with a polymer to form MMMs with enhanced ethylene/ethane

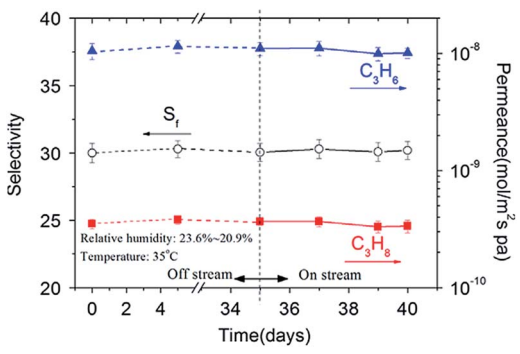

Fig. 20 Off-stream stability and on-stream stability test of C_3H_6/C_3H_8 mixture permeances on the ZIF-8 membrane at 35 °C. (Reprinted with permission from ref. 67. Copyright 2014 Elsevier.)

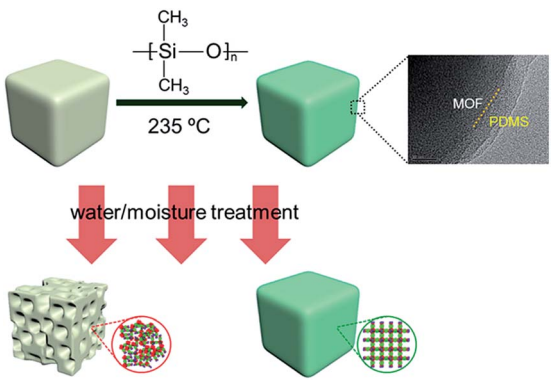

Fig. 21 Schematic of PDMS-coating on the surface of MOFs and improvement of the moisture/water resistance of MOFs. (Reprinted with permission from ref. 153. Copyright 2016 American Chemical Society.)

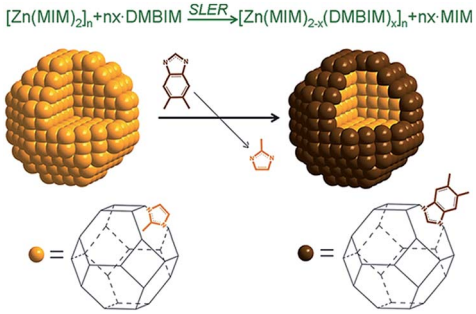

Fig. 22 Schematic of the shell-ligand-exchange-reaction (SLER) process of ZIF-8. (Reprinted with permission from ref. 44. Copyright 2013 RSC.)

separation performance.[68] Because of the interaction between MOF particles and the polymer matrix, the involvement of the MOF fillers can reduce the polymer chain mobility to enhance the plasticization resistance of the obtained membranes.

Summary and outlook

MOF membranes for gas separation represent an important and rapidly expanding research area for gas separation. The choices of structure design and growth strategies are critical for obtaining the membrane with ideal properties. This review summarizes the recent developments in MOF membranes, focused on membrane performance improvement and resolutions to the problems of practical applications. Ultrathin membranes are preferred for their higher permeance. Owing to the development of 2D materials in the separation area, building 2D MOF membranes has become a great challenge. So far, 2D MOF nanosheets can be successfully fabricated by both "top-down" and "bottom-up" approaches. These 2D MOF nanosheets have then been used as building blocks to prepare pure MOF membranes or MOF membranes combined with polymers to synthesize MMMs. Besides 2D MOFs, other 2D materials, such as GO, can also be used as a template to make 3D MOFs into a 2D morphology. Another key factor that affects the membrane performance is the separation selectivity. Aiming to increase membrane selectivity, the advantage of MOF materials design can give solutions in different directions. The two parts that build the MOF framework, *i.e.*, the metal centers and organic ligands, are facile to be varied to adjust the pore size and environment, which can fit the molecular size of a specific gas mixture to achieve molecule sieving. Furthermore, the channels of MOF membranes can also be fine tailored by embedding guest molecules. In addition to the MOF material itself, a variety of other species have been introduced into the MOF membrane as precursors, inserts, and repairing agents to enhance the performance of the original membrane. Although the separation performances of MOF membranes have been improved by the methods mentioned above, some important issues still need to be addressed, such as their stability and scale-up fabrication with acceptable cost. MMMs are supposed to be a solution to the scale-up issue with viable trade-offs in a short-term solution, especially for hollow fibers with an asymmetric structure. Hollow fibers are picked as the support to grow MOF membranes on the inner side by the diffusion method. This membrane-processing approach is a notable step toward realizing the scalable molecular sieving of MOF membranes. Other novel methods and techniques may also be well prepared for MOF membrane scale-up, such as electrospinning, electrospray deposition, hot-pressing and photoinduced postsynthetic polymerization, *etc.* To resolve the stability issue of MOF membranes, the development of MOFs with robust structures is chosen as a direct strategy. Some famous frameworks, such as the ZIF series and UIO series, have been prepared into membranes to test their performances under high temperature and humid conditions. For MOF membranes with low stability, some reinforcement strategies can be taken to enhance their stability. Ligands and metal centers exchange are effective in enhancing the steadiness, while a protective coating is also useful to enhance the hydrophobicity of MOF membranes.

In addition to the recent research progress we have discussed, new research related to MOF membranes has been reported for separation applications. Tomographic FIB-SEM may be a powerful technique to assess the spatial distribution of MOF fillers,[156] the polymer, and the void space in the membrane in 3D. When combined with image analysis, it provides a convenient method to quantify the filler–matrix contact, which is an essential feature for the performance of MMMs. The precise and quantitative insight into the key structural features in the nanoscale range offers feed-back to the membrane casting process. Therefore, it represents an important progress toward the rational design of MMMs with enhanced structural features and separation performance.

Thus, it will be fantastic to have a membrane combining the ease of processing of polymers and the ordered pore structure of MOFs. Beyond MOFs, some crystal materials constituted by reversible bonds have similar unique pore sizes as MOFs and can be dissolved in the solution and recrystallized into the membrane. In the work reported by Prof. Wu, polyanionic clusters as connection nodes and cationic pseudorotaxanes acting as bridging monomers were connected, giving a single-layer ionic self-assembled framework.[157] The single layer with a uniform mesh-like structure was dispersed in aqueous solution and filtrated on the porous substrate into the membrane to sieve quantum dots within 0.1 nm. The soft supramolecular polymer framework is promising for the separation of gas molecules due to its advantage of a uniform pore size, 2D flexible structure, and solution processability.

Turning the perspective from 2D to 0D, Prof. Cooper *et al.* demonstrated that porous organic cages (POCs) could be solution-processed into coherent thin films with a tunable structure and porosity.[158] As shown in Fig. 23, POCs with a designated structure were dissolved in the solution like polymers and dispersed on the substrates *via* spin-coating. By varying the speed of spinning and the concentration of the cage molecules in solution, POC membranes with different thicknesses were obtained after the solvent evaporation. Due to their advantage of solution processability, these POC materials with

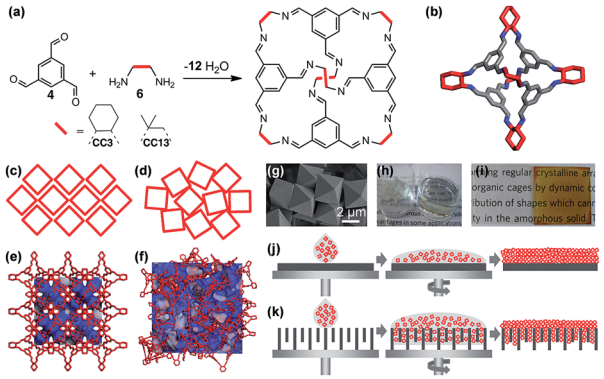

Fig. 23 Synthesis of POCs and the solution-processing of POCs into thin films. (a) Synthetic pathways and chemical structures of POCs. (b) 3D crystalline structure of the CC3 cage. (c) Schemes showing the ordered assembly of cage molecules into crystals, and (d) the disordered packing of cage molecules in the amorphous state. Molecular simulation of (e) crystalline structure and (f) amorphous packing of the cage CC3. (g) SEM image of CC3 crystals, (h) photograph of crystalline CC3 cage solids (left) and solution of cage molecules dissolved in solvent (right), (i) photograph of cage thin films spin-coated on glass slides (left: transparent cage film coated on glass alone, right: cage film stained with iodine). (j and k) Scheme illustrating spin-coating of the cage solution into an ultrathin layer of cage films on (j) a nonporous substrate, and (k) a porous substrate, forming a thin-film composite membrane with a molecular sieving function. (Reprinted with permission from ref. 158. Copyright 2016 Nature publishing group.)

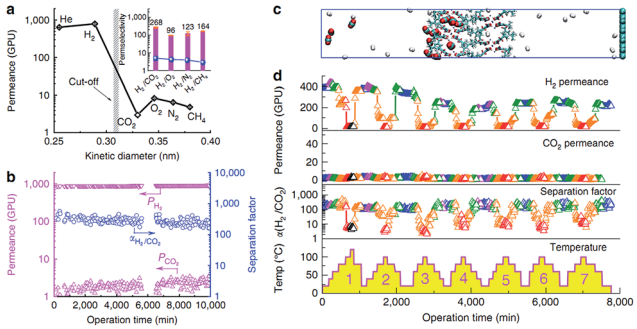

Fig. 24 (a) Single-gas permeation of a 40 nm membrane. (b) A 10 000 min continuous test of a 40 nm membrane for the separation of an equimolar H_2/CO_2 mixture at room temperature. (c) A snapshot of MD simulation for the separation of an equimolar H_2/CO_2 mixture through a bilayered MAMS-1 membrane. (d) Gas permeance and H_2/CO_2 separation factors of a 40 nm membrane under seven heating/cooling cycles. (Reprinted with permission from ref. 69. Copyright 2016 Nature publishing group.)

unique pore size are attractive to be prepared into large-scale membranes for gas separation. However, the stability issue should be addressed when the POC membrane is applied in a practical process. Post-reinforcement of POC membranes, more robust cages for membrane preparation, and POC-based MMMs may be the future research focuses of this kind of membrane.[159]

Furthermore, the gating-open effect of the channels in some MOF materials is another advantage for gas separation.[160–166] It has been demonstrated that the gas adsorption property can benefit from the flexibility of the framework. Involving this property into membrane separation will allow gas permeation to be adjusted by changing the operating conditions, such as temperature, pressure, even light and electrical stimulation. A mixture of three or more gases can be separated stepwise by using a condition switching program on a single membrane, which could be called a "smart membrane" and is effective for the separation process. However, this will be a challenging topic as the crystal may crack at the micro level during the gate opening/closing process. Several groups are working on this direction presently and in the work reported by Heinke and co-workers, a MOF membrane based on the azobenzene side-groups was reported.[167] Under irradiation with ultraviolet or visible light, the azobenzene moieties can be switched from the *trans* to the *cis* configuration, leading to a changing pore size and gas separation selectivity. In a very recent research, Zhao reported a reversed thermo-switchable molecular sieving membrane composed of 2D MOF nanosheets for H_2/CO_2 separation, combining the advantages of flexibility and an ultrathin membrane.[69] As illustrated in Fig. 24, the 40 nm membrane in that study exhibited an adjustable gas separation performance corresponding to the operation temperature. The freely rotated *tert*-butyl groups in the framework is the key point for the thermo-switchable separation behavior, characterized by *in situ* variable temperature PXRD.

The separation of mixtures without using heat would change the world in terms of lower energy consumption and pollution.[1] Compared with other porous materials, the multifunction group, tunable pore size, and flexible framework make MOF-based membranes promising materials for some of the crucial gas separations, such as hydrocarbons separation and CO_2 capture (pre-combustion and post-combustion). Based on the crystal engineering, large numbers of MOF structures with different surface chemistries and pore sizes have been added into the candidate database, which is an advance and challenging aspect. Preparation and performance studies have been done widely on some famous and promising MOFs, such as the ZIFs series.[117] More potential MOFs with low-cost ligands, scale-up preparation methods, stable and suitable structures will be found and selected from the database, and computational studies may play the role of a guide for effective seeking good candidates.

Acknowledgements

This work was financially supported by the NSFC (Grant No. 21501198, 21601205, 21371179, 21271117), Taishan Scholar Foundation (ts201511019), and the Fundamental Research Funds for the Central Universities (13CX05010A, 15CX02069A). Sincere gratitude goes to M. Zhang and Q. Xu for the advice of writing and artwork.

Notes and references

1 D. S. Sholl and R. P. Lively, *Nature*, 2016, **532**, 435–437.
2 J. Y. S. Lin, *Science*, 2016, **353**, 121–122.

3 F. Gallucci, E. Fernandez, P. Corengia and M. van Sint Annaland, *Chem. Eng. Sci.*, 2013, **92**, 40–66.
4 A. R. Smith and J. Klosek, *Fuel Process. Technol.*, 2001, **70**, 115–134.
5 H. Q. Lin, E. Van Wagner, R. Raharjo, B. D. Freeman and I. Roman, *Adv. Mater.*, 2006, **18**, 39–44.
6 J. T. Vaughn and W. J. Koros, *J. Membr. Sci.*, 2014, **465**, 107–116.
7 K. Ramasubramanian, Y. Zhao and W. S. Winston Ho, *AIChE J.*, 2013, **59**, 1033–1045.
8 C. A. Scholes, G. W. Stevens and S. E. Kentish, *Fuel*, 2012, **96**, 15–28.
9 E. D. Bloch, W. L. Queen, R. Krishna, J. M. Zadrozny, C. M. Brown and J. R. Long, *Science*, 2012, **335**, 1606–1610.
10 R. W. Baker, *Membrane Technology and Applications*, John Wiley & Sons, Ltd., Newark, California, 3rd edn, 2012.
11 N. Kosinov, J. Gascon, F. Kapteijn and E. J. M. Hensen, *J. Membr. Sci.*, 2016, **499**, 65–79.
12 R. W. Baker, *Ind. Eng. Chem. Res.*, 2002, **41**, 1393–1411.
13 A. F. Ismail and L. I. B. David, *J. Membr. Sci.*, 2001, **193**, 1–18.
14 D. L. Gin and R. D. Noble, *Science*, 2011, **332**, 674–676.
15 D. E. Sanders, Z. P. Smith, R. Guo, L. M. Robeson, J. E. McGrath, D. R. Paul and B. D. Freeman, *Polymer*, 2013, **54**, 4729–4761.
16 L. M. Robeson, *J. Membr. Sci.*, 2008, **320**, 390–400.
17 B. D. Freeman, *Macromolecules*, 1999, **32**, 375–380.
18 P. Tung Cao Thanh, H. S. Kim and K. B. Yoon, *Science*, 2011, **334**, 1533–1538.
19 J. Coronas and J. Santamaría, *Sep. Purif. Rev.*, 1999, **28**, 127–177.
20 W. J. Koros, Y. H. Ma and T. Shimidzu, *Pure Appl. Chem.*, 1996, **68**, 1479–1489.
21 A. Huang and J. Caro, *Chem. Commun.*, 2010, **46**, 7748–7750.
22 H. Furukawa, K. E. Cordova, M. O'Keeffe and O. M. Yaghi, *Science*, 2013, **341**, 1230444.
23 S. Zhou, X. Zou, F. Sun, F. Zhang, S. Fan, H. Zhao, T. Schiestel and G. Zhu, *J. Mater. Chem.*, 2012, **22**, 10322.
24 J. Nan, X. Dong, W. Wang, W. Jin and N. Xu, *Langmuir*, 2011, **27**, 4309–4312.
25 Y. Liu, G. Zeng, Y. Pan and Z. Lai, *J. Membr. Sci.*, 2011, **379**, 46–51.
26 A. Huang and J. Caro, *Angew. Chem., Int. Ed.*, 2011, **50**, 4979–4982.
27 H. Bux, C. Chmelik, R. Krishna and J. Caro, *J. Membr. Sci.*, 2011, **369**, 284–289.
28 Y. Li, F. Liang, H. Bux, W. Yang and J. Caro, *J. Membr. Sci.*, 2010, **354**, 48–54.
29 A. Huang, W. Dou and J. Caro, *J. Am. Chem. Soc.*, 2010, **132**, 15562–15564.
30 A. Huang, H. Bux, F. Steinbach and J. Caro, *Angew. Chem., Int. Ed.*, 2010, **49**, 4958–4961.
31 Y. Yoo, Z. Lai and H.-K. Jeong, *Microporous Mesoporous Mater.*, 2009, **123**, 100–106.
32 S. R. Venna and M. A. Carreon, *J. Am. Chem. Soc.*, 2009, **132**, 76–78.
33 H. Guo, G. Zhu, I. J. Hewitt and S. Qiu, *J. Am. Chem. Soc.*, 2009, **131**, 1646–1647.
34 J. R. Li, R. J. Kuppler and H. C. Zhou, *Chem. Soc. Rev.*, 2009, **38**, 1477–1504.
35 D. Zacher, O. Shekhah, C. Wöll and R. A. Fischer, *Chem. Soc. Rev.*, 2009, **38**, 1418–1429.
36 N. Rangnekar, N. Mittal, B. Elyassi, J. Caro and M. Tsapatsis, *Chem. Soc. Rev.*, 2015, **44**, 7128–7154.
37 I. Erucar, G. Yilmaz and S. Keskin, *Chem.–Asian J.*, 2013, **8**, 1692–1704.
38 S. Qiu, M. Xue and G. Zhu, *Chem. Soc. Rev.*, 2014, **43**, 6116–6140.
39 C. Wang, X. Liu, N. Keser Demir, J. P. Chen and K. Li, *Chem. Soc. Rev.*, 2016, **45**, 5107–5134.
40 Y. L. Yuan Peng, Y. Ban, H. Jin, W. Jiao, X. Liu and W. Yang, *Science*, 2014, **346**, 1356–1359.
41 Y. Ban, Z. Li, Y. Li, Y. Peng, H. Jin, W. Jiao, A. Guo, P. Wang, Q. Yang, C. Zhong and W. Yang, *Angew. Chem., Int. Ed.*, 2015, **54**, 15483–15487.
42 J. Fu, S. Das, G. Xing, T. Ben, V. Valtchev and S. Qiu, *J. Am. Chem. Soc.*, 2016, **138**, 7673–7680.
43 A. J. Brown, N. A. Brunelli, K. Eum, F. Rashidi, J. R. Johnson, W. J. Koros, C. W. Jones and S. Nair, *Science*, 2014, **345**, 72–75.
44 X. Liu, Y. Li, Y. Ban, Y. Peng, H. Jin, H. Bux, L. Xu, J. Caro and W. Yang, *Chem. Commun.*, 2013, **49**, 9140–9142.
45 S. Kitagawa, R. Kitaura and S. Noro, *Angew. Chem., Int. Ed.*, 2004, **43**, 2334–2375.
46 T. Rodenas, I. Luz, G. Prieto, B. Seoane, H. Miro, A. Corma, F. Kapteijn, F. X. Llabres i Xamena and J. Gascon, *Nat. Mater.*, 2015, **14**, 48–55.
47 Z. Kang, Y. Peng, Z. Hu, Y. Qian, C. Chi, L. Y. Yeo, L. Tee and D. Zhao, *J. Mater. Chem. A*, 2015, **3**, 20801–20810.
48 Y. Hu, J. Wei, Y. Liang, H. Zhang, X. Zhang, W. Shen and H. Wang, *Angew. Chem., Int. Ed.*, 2016, **55**, 2048–2052.
49 A. Bétard, H. Bux, S. Henke, D. Zacher, J. Caro and R. A. Fischer, *Microporous Mesoporous Mater.*, 2012, **150**, 76–82.
50 Z. Kang, M. Xue, L. Fan, L. Huang, L. Guo, G. Wei, B. Chen and S. Qiu, *Energy Environ. Sci.*, 2014, **7**, 4053–4060.
51 W. Li, Y. Zhang, C. Zhang, Q. Meng, Z. Xu, P. Su, Q. Li, C. Shen, Z. Fan, L. Qin and G. Zhang, *Nat. Commun.*, 2016, **7**, 11315.
52 H. T. Kwon, H. K. Jeong, A. S. Lee, H. S. An and J. S. Lee, *J. Am. Chem. Soc.*, 2015, **137**, 12304–12311.
53 A. Huang, Q. Liu, N. Wang and J. Caro, *Microporous Mesoporous Mater.*, 2014, **192**, 18–22.
54 N. Wang, A. Mundstock, Y. Liu, A. Huang and J. Caro, *Chem. Eng. Sci.*, 2015, **124**, 27–36.
55 Z. Kang, L. Fan, S. Wang, D. Sun, M. Xue and S. Qiu, *CrystEngComm*, 2017, **19**, 1601–1606.
56 Y. Liu, N. Wang, J. H. Pan, F. Steinbach and J. Caro, *J. Am. Chem. Soc.*, 2014, **136**, 14353–14356.
57 M. Drobek, M. Bechelany, C. Vallicari, A. Abou Chaaya, C. Charmette, C. Salvador-Levehang, P. Miele and A. Julbe, *J. Membr. Sci.*, 2015, **475**, 39–46.

58 Y. Mao, L. shi, H. Huang, W. Cao, J. Li, L. Sun, X. Jin and X. Peng, *Chem. Commun.*, 2013, **49**, 5666–5668.
59 A. Huang, Q. Liu, N. Wang, Y. Zhu and J. Caro, *J. Am. Chem. Soc.*, 2014, **136**, 14686–14689.
60 C. Zhang, K. Zhang, L. Xu, Y. Labreche, B. Kraftschik and W. J. Koros, *AIChE J.*, 2014, **60**, 2625–2635.
61 F. Cacho-Bailo, S. Catalán-Aguirre, M. Etxeberría-Benavides, O. Karvan, V. Sebastian, C. Téllez and J. Coronas, *J. Membr. Sci.*, 2015, **476**, 277–285.
62 F. Cacho-Bailo, G. Caro, M. Etxeberria-Benavides, O. Karvan, C. Tellez and J. Coronas, *Chem. Commun.*, 2015, **51**, 11283–11285.
63 L. Fan, M. Xue, Z. Kang, H. Li and S. Qiu, *J. Mater. Chem.*, 2012, **22**, 25272–25276.
64 V. M. Aceituno Melgar, H. T. Kwon and J. Kim, *J. Membr. Sci.*, 2014, **459**, 190–196.
65 O. Shekhah, R. Swaidan, Y. Belmabkhout, M. du Plessis, T. Jacobs, L. J. Barbour, I. Pinnau and M. Eddaoudi, *Chem. Commun.*, 2014, **50**, 2089–2092.
66 S. Hurrle, S. Friebe, J. Wohlgemuth, C. Wöll, J. Caro and L. Heinke, *Chem.–Eur. J.*, 2017, **23**, 2294–2298.
67 D. Liu, X. Ma, H. Xi and Y. S. Lin, *J. Membr. Sci.*, 2014, **451**, 85–93.
68 J. E. Bachman, Z. P. Smith, T. Li, T. Xu and J. R. Long, *Nat. Mater.*, 2016, **15**, 845–849.
69 X. Wang, C. Chi, K. Zhang, Y. Qian, K. M. Gupta, Z. Kang, J. Jiang and D. Zhao, *Nat. Commun.*, 2017, **8**, 14460.
70 B. Mi, *Science*, 2014, **343**, 740–742.
71 Y. Li and W. Yang, *Chin. J. Catal.*, 2015, **36**, 692–697.
72 H. Li, Z. Song, X. Zhang, Y. Huang, S. Li, Y. Mao, H. J. Ploehn, Y. Bao and M. Yu, *Science*, 2013, **342**, 95–98.
73 A. Galve, D. Sieffert, E. Vispe, C. Téllez, J. Coronas and C. Staudt, *J. Membr. Sci.*, 2011, **370**, 131–140.
74 W.-g. Kim and S. Nair, *Chem. Eng. Sci.*, 2013, **104**, 908–924.
75 Z. Zheng, R. Grunker and X. Feng, *Adv. Mater.*, 2016, **28**, 6529–6545.
76 M. Tsapatsis, *Science*, 2011, **334**, 767–768.
77 Z. Zhong, J. Yao, R. Chen, Z. Low, M. He, J. Z. Liu and H. Wang, *J. Mater. Chem. A*, 2015, **3**, 15715–15722.
78 J. Choi and M. Tsapatsis, *J. Am. Chem. Soc.*, 2010, **132**, 448–449.
79 K. Varoon, X. Zhang, B. Elyassi, D. D. Brewer, M. Gettel, S. Kumar, J. A. Lee, S. Maheshwari, A. Mittal, C. Y. Sung, M. Cococcioni, L. F. Francis, A. V. McCormick, K. A. Mkhoyan and M. Tsapatsis, *Science*, 2011, **334**, 72–75.
80 H. K. Jeong, S. Nair, T. Vogt, L. C. Dickinson and M. Tsapatsis, *Nat. Mater.*, 2003, **2**, 53–58.
81 Z. P. Lai, G. Bonilla, I. Diaz, J. G. Nery, K. Sujaoti, M. A. Amat, E. Kokkoli, O. Terasaki, R. W. Thompson, M. Tsapatsis and D. G. Vlachos, *Science*, 2003, **300**, 456–460.
82 N. Eng-Poh, D. Chateigner, T. Bein, V. Valtchev and S. Mintova, *Science*, 2012, **335**, 70–73.
83 D. N. Bunck and W. R. Dichtel, *J. Am. Chem. Soc.*, 2013, **135**, 14952–14955.
84 P.-Z. Li, Y. Maeda and Q. Xu, *Chem. Commun.*, 2011, **47**, 8436–8438.
85 P. Amo-Ochoa, L. Welte, R. Gonzalez-Prieto, P. J. Sanz Miguel, C. J. Gomez-Garcia, E. Mateo-Marti, S. Delgado, J. Gomez-Herrero and F. Zamora, *Chem. Commun.*, 2010, **46**, 3262–3264.
86 V. Valtchev and L. Tosheva, *Chem. Rev.*, 2013, **113**, 6734–6760.
87 T. Tsuruoka, S. Furukawa, Y. Takashima, K. Yoshida, S. Isoda and S. Kitagawa, *Angew. Chem., Int. Ed.*, 2009, **48**, 4739–4743.
88 T. M. Nenoff, *Nat. Chem.*, 2015, **7**, 377–378.
89 H. Chun, D. N. Dybtsev, H. Kim and K. Kim, *Chem.–Eur. J.*, 2005, **11**, 3521–3529.
90 P. Tung Cao Thanh, H. S. Kim and K. B. Yoon, *Science*, 2011, **334**, 1533–1538.
91 X. Cui, K. Chen, H. Xing, Q. Yang, R. Krishna, Z. Bao, H. Wu, W. Zhou, X. Dong, Y. Han, B. Li, Q. Ren, M. J. Zaworotko and B. Chen, *Science*, 2016, **353**, 141–144.
92 A. Cadiau, K. Adil, P. M. Bhatt, Y. Belmabkhout and M. Eddaoudi, *Science*, 2016, **353**, 137–140.
93 R. Banerjee, A. Phan, B. Wang, C. Knobler, H. Furukawa, M. O'Keeffe and O. M. Yaghi, *Science*, 2008, **319**, 939–943.
94 M. Eddaoudi, J. Kim, N. Rosi, D. Vodak, J. Wachter, M. O'Keeffe and O. M. Yaghi, *Science*, 2002, **295**, 469–472.
95 A. Huang, Y. Chen, Q. Liu, N. Wang, J. Jiang and J. Caro, *J. Membr. Sci.*, 2014, **454**, 126–132.
96 J. A. Thompson, C. R. Blad, N. A. Brunelli, M. E. Lydon, R. P. Lively, C. W. Jones and S. Nair, *Chem. Mater.*, 2012, **24**, 1930–1936.
97 K. Eum, K. C. Jayachandrababu, F. Rashidi, K. Zhang, J. Leisen, S. Graham, R. P. Lively, R. R. Chance, D. S. Sholl, C. W. Jones and S. Nair, *J. Am. Chem. Soc.*, 2015, **137**, 4191–4197.
98 F. Rashidi, C. R. Blad, C. W. Jones and S. Nair, *AIChE J.*, 2016, **62**, 525–537.
99 C. K. Brozek and M. Dinca, *Chem. Soc. Rev.*, 2014, **43**, 5456–5467.
100 E. J. Kyprianidou, T. Lazarides, S. Kaziannis, C. Kosmidis, G. Itskos, M. J. Manos and A. J. Tasiopoulos, *J. Mater. Chem. A*, 2014, **2**, 5258–5266.
101 P. Shen, W.-W. He, D.-Y. Du, H.-L. Jiang, S.-L. Li, Z.-L. Lang, Z.-M. Su, Q. Fua and Y.-Q. Lan, *Chem. Sci.*, 2014, **5**, 1368–1374.
102 P. H. Jia Li, X.-R. Wu, J. Tao, R.-B. Huang and L.-S. Zheng, *Chem. Sci.*, 2013, **4**, 3232–3238.
103 K. Xu, C. Yuan, J. Caro and A. Huang, *J. Membr. Sci.*, 2016, **511**, 1–8.
104 G. Guan, K. Kusakabe and S. Morooka, *Sep. Sci. Technol.*, 2001, **36**, 2233–2245.
105 K. Sumida, D. L. Rogow, J. A. Mason, T. M. McDonald, E. D. Bloch, Z. R. Herm, T. H. Bae and J. R. Long, *Chem. Rev.*, 2012, **112**, 724–781.
106 W. Wang, X. Dong, J. Nan, W. Jin, Z. Hu, Y. Chen and J. Jiang, *Chem. Commun.*, 2012, **48**, 7022–7024.
107 Z. Kang, M. Xue, L. Fan, J. Ding, L. Guo, L. Gao and S. Qiu, *Chem. Commun.*, 2013, **49**, 10569–10571.
108 Y. Mao, J. Li, W. Cao, Y. Ying, P. Hu, Y. Liu, L. Sun, H. Wang, C. Jin and X. Peng, *Nat. Commun.*, 2014, **5**, 5532.

109 J. Li, W. Cao, Y. Mao, Y. Ying, L. Sun and X. Peng, *CrystEngComm*, 2014, **16**, 9788–9791.
110 I. Kiesow, D. Marczewski, L. Reinhardt, M. Mühlmann, M. Possiwan and W. A. Goedel, *J. Am. Chem. Soc.*, 2013, **135**, 4380–4388.
111 X. Wang, C. Chi, J. Tao, Y. Peng, S. Ying, Y. Qian, J. Dong, Z. Hu, Y. Gu and D. Zhao, *Chem. Commun.*, 2016, **52**, 8087–8090.
112 A. Betard and R. A. Fischer, *Chem. Rev.*, 2012, **112**, 1055–1083.
113 J. Caro, *Procedia Eng.*, 2012, **44**, 1–2.
114 M. Shah, M. C. McCarthy, S. Sachdeva, A. K. Lee and H.-K. Jeong, *Ind. Eng. Chem. Res.*, 2012, **51**, 2179–2199.
115 J. Gascon and F. Kapteijn, *Angew. Chem., Int. Ed.*, 2010, **49**, 1530–1532.
116 E. Adatoz, A. K. Avci and S. Keskin, *Sep. Purif. Technol.*, 2015, **152**, 207–237.
117 V. M. Aceituno Melgar, J. Kim and M. R. Othman, *J. Ind. Eng. Chem.*, 2015, **28**, 1–15.
118 L. Xu, M. Rungta and W. J. Koros, *J. Membr. Sci.*, 2011, **380**, 138–147.
119 D. Q. Vu, W. J. Koros and S. J. Miller, *J. Membr. Sci.*, 2003, **211**, 311–334.
120 J. Liu, T.-H. Bae, W. Qiu, S. Husain, S. Nair, C. W. Jones, R. R. Chance and W. J. Koros, *J. Membr. Sci.*, 2009, **343**, 157–163.
121 S. Husain and W. J. Koros, *J. Membr. Sci.*, 2007, **288**, 195–207.
122 J. A. Thompson, K. W. Chapman, W. J. Koros, C. W. Jones and S. Nair, *Microporous Mesoporous Mater.*, 2012, **158**, 292–299.
123 C. Zhang, Y. Dai, J. R. Johnson, O. Karvan and W. J. Koros, *J. Membr. Sci.*, 2012, **389**, 34–42.
124 J. Ploegmakers, S. Japip and K. Nijmeijer, *J. Membr. Sci.*, 2013, **428**, 445–453.
125 Y. Pan, T. Li, G. Lestari and Z. Lai, *J. Membr. Sci.*, 2012, **390**, 93–98.
126 M. J. C. Ordonez, K. J. Balkus Jr, J. P. Ferraris and I. H. Musselman, *J. Membr. Sci.*, 2010, **361**, 28–37.
127 T. Li, Y. Pan, K.-V. Peinemann and Z. Lai, *J. Membr. Sci.*, 2013, **425**, 235–242.
128 Y. Dai, J. R. Johnson, O. Karvan, D. S. Sholl and W. J. Koros, *J. Membr. Sci.*, 2012, **401**, 76–82.
129 A. F. Ismail, T. D. Kusworo and A. Mustafa, *J. Membr. Sci.*, 2008, **319**, 306–312.
130 W. J. Koros and G. K. Fleming, *J. Membr. Sci.*, 1993, **83**, 1–80.
131 M. G. Buonomenna, *RSC Adv.*, 2013, **3**, 5694–5740.
132 J. Choi, H.-K. Jeong, M. A. Snyder, J. A. Stoeger, R. I. Masel and M. Tsapatsis, *Science*, 2009, **325**, 590–593.
133 M. Tsapatsis, *Science*, 2011, **334**, 767–768.
134 T. C. T. Pham, H. S. Kim and K. B. Yoon, *Science*, 2011, **334**, 1533–1538.
135 A. J. Brown, J. R. Johnson, M. E. Lydon, W. J. Koros, C. W. Jones and S. Nair, *Angew. Chem., Int. Ed.*, 2012, **51**, 10615–10618.
136 L. Fan, M. Xue, Z. Kang and S. Qiu, *Sci. China: Chem.*, 2013, **56**, 459–464.
137 V. Chernikova, O. Shekhah and M. Eddaoudi, *ACS Appl. Mater. Interfaces*, 2016, **8**, 20459–20464.
138 O. Shekhah, H. Wang, S. Kowarik, F. Schreiber, M. Paulus, M. Tolan, C. Sternemann, F. Evers, D. Zacher, R. A. Fischer and C. Wöll, *J. Am. Chem. Soc.*, 2007, **129**, 15118–15119.
139 J.-L. Zhuang, A. Terfort and C. Wöll, *Coord. Chem. Rev.*, 2016, **307**, 391–424.
140 O. Shekhah and M. Eddaoudi, *Chem. Commun.*, 2013, **49**, 10079–10081.
141 O. Shekhah, K. Hirai, H. Wang, H. Uehara, M. Kondo, S. Diring, D. Zacher, R. A. Fischer, O. Sakata, S. Kitagawa, S. Furukawa and C. Woell, *Dalton Trans.*, 2011, **40**, 4954–4958.
142 O. Shekhah, H. Wang, M. Paradinas, C. Ocal, B. Schuepbach, A. Terfort, D. Zacher, R. A. Fischer and C. Woell, *Nat. Mater.*, 2009, **8**, 481–484.
143 Y. Chen, S. Li, X. Pei, J. Zhou, X. Feng, S. Zhang, Y. Cheng, H. Li, R. Han and B. Wang, *Angew. Chem., Int. Ed.*, 2015, **55**, 3419–3423.
144 Y. Chen, S. Zhang, S. Cao, S. Li, F. Chen, S. Yuan, C. Xu, J. Zhou, X. Feng, X. Ma and B. Wang, *Adv. Mater.*, 2017, DOI: 10.1002/adma.201606221.
145 Y. Zhang, X. Feng, H. Li, Y. Chen, J. Zhao, S. Wang, L. Wang and B. Wang, *Angew. Chem., Int. Ed.*, 2015, **54**, 4259–4263.
146 K. A. Cychosz and A. J. Matzger, *Langmuir*, 2010, **26**, 17198–17202.
147 J. J. Low, A. I. Benin, P. Jakubczak, J. F. Abrahamian, S. A. Faheem and R. R. Willis, *J. Am. Chem. Soc.*, 2009, **131**, 15834–15842.
148 G. Ferey, C. Mellot-Draznieks, C. Serre, F. Millange, J. Dutour, S. Surble and I. Margiolaki, *Science*, 2005, **309**, 2040–2042.
149 D. Feng, Z.-Y. Gu, J.-R. Li, H.-L. Jiang, Z. Wei and H.-C. Zhou, *Angew. Chem., Int. Ed.*, 2012, **51**, 10307–10310.
150 J. H. Cavka, S. Jakobsen, U. Olsbye, N. Guillou, C. Lamberti, S. Bordiga and K. P. Lillerud, *J. Am. Chem. Soc.*, 2008, **130**, 13850–13851.
151 V. Colombo, S. Galli, H. J. Choi, G. D. Han, A. Maspero, G. Palmisano, N. Masciocchi and J. R. Long, *Chem. Sci.*, 2011, **2**, 1311–1319.
152 J. B. Decoste, G. W. Peterson, M. W. Smith, C. A. Stone and C. R. Willis, *J. Am. Chem. Soc.*, 2012, **134**, 1486–1489.
153 W. Zhang, Y. Hu, J. Ge, H. L. Jiang and S. H. Yu, *J. Am. Chem. Soc.*, 2014, **136**, 16978–16981.
154 X. Liu, N. K. Demir, Z. Wu and K. Li, *J. Am. Chem. Soc.*, 2015, **137**, 6999–7002.
155 Z. Kang, S. Wang, L. Fan, Z. Xiao, R. Wang and D. Sun, *Mater. Lett.*, 2017, **189**, 82–85.
156 T. Rodenas, M. van Dalen, E. García-Pérez, P. Serra-Crespo, B. Zornoza, F. Kapteijn and J. Gascon, *Adv. Funct. Mater.*, 2014, **24**, 249–256.
157 L. Yue, S. Wang, D. Zhou, H. Zhang, B. Li and L. Wu, *Nat. Commun.*, 2016, **7**, 10742.
158 Q. Song, S. Jiang, T. Hasell, M. Liu, S. Sun, A. K. Cheetham, E. Sivaniah and A. I. Cooper, *Adv. Mater.*, 2016, **28**, 2629–2637.
159 T. Hasell and A. I. Cooper, *Nat. Rev. Mater.*, 2016, **1**, 16053.

160 R. Kitaura, K. Seki, G. Akiyama and S. Kitagawa, *Angew. Chem., Int. Ed.*, 2003, **42**, 428–431.
161 Z. Chang, D. H. Yang, J. Xu, T. L. Hu and X. H. Bu, *Adv. Mater.*, 2015, **27**, 5432–5441.
162 S. Ma, D. Sun, X.-S. Wang and H.-C. Zhou, *Angew. Chem., Int. Ed.*, 2007, **46**, 2458–2462.
163 S. S. Mondal, A. Bhunia, I. A. Baburin, C. Jager, A. Kelling, U. Schilde, G. Seifert, C. Janiak and H. J. Holdt, *Chem. Commun.*, 2013, **49**, 7599–7601.
164 M. L. Foo, R. Matsuda, Y. Hijikata, R. Krishna, H. Sato, S. Horike, A. Hori, J. Duan, Y. Sato, Y. Kubota, M. Takata and S. Kitagawa, *J. Am. Chem. Soc.*, 2016, **138**, 3022–3030.
165 N. Nijem, H. Wu, P. Canepa, A. Marti, K. J. Balkus Jr, T. Thonhauser, J. Li and Y. J. Chabal, *J. Am. Chem. Soc.*, 2012, **134**, 15201–15204.
166 S. Sakaida, K. Otsubo, O. Sakata, C. Song, A. Fujiwara, M. Takata and H. Kitagawa, *Nat. Chem.*, 2016, **8**, 377–383.
167 Z. Wang, A. Knebel, S. Grosjean, D. Wagner, S. Bräse, C. Wöll, J. Caro and L. Heinke, *Nat. Commun.*, 2016, **7**, 13872.